

# Surface Temperature Changes due to Aerosols using Satellite Observations over India.



A **thesis** submitted towards partial fulfilment of  
BS-MS dual degree program  
*by*

**Sarin TS**  
(20161197)

Under the guidance of

**Dr V Vinoj.**

School of Earth, Ocean, and Climate Sciences  
Indian Institute of Technology, Bhubaneswar

*to the*

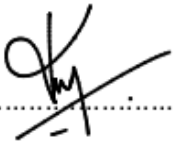
Department of Earth and Climate Science  
Indian Institute of Science Education and Research, Pune

June 04<sup>th</sup>, 2021

All rights reserved

## Certificate.

This is to certify that this dissertation entitled “**Surface Temperature Changes associated with Aerosols using Satellite Observations over India**” towards the partial fulfilment of the BS-MS dual degree program at the Indian Institute of Science Education and Research, Pune represents original research carried out by **Sarin TS (20161197)**, at the Indian Institute of Technology, Bhubaneswar under the supervision of **Dr V Vinoj** (Assistant Professor, School of Earth, Ocean and Climate Sciences, Indian Institute of Technology Bhubaneswar) during the academic year 2020-2021.

Supervisor .....  


(Dr. V Vinoj)

Expert Member.....

(Dr Suhas Ettammal)

Committee .....

## Declaration

I hereby declare that the matter embodied in the report entitled “**Surface Temperature Changes associated with Aerosols using Satellite Observations Over India**” are the results of the work carried out by me at the School of Earth Ocean and Climate Sciences, Indian Institute of Technology, under the supervision of **Dr V Vinoj** (Assistant Professor, School of Earth, Ocean and Climate Sciences, Indian Institute of Technology Bhubaneswar) and the same has not been submitted elsewhere for any other degree.



**Sarin TS.**

**04<sup>th</sup> June 2021.**

## **Acknowledgements.**

I would like to express my sincere thanks to Dr V. Vinoj, Assistant Professor, IIT Bhubaneswar, for his meaningful assistance, tireless guidance, patience, and support. Thank you for always being so approachable and for entertaining my questions. Special thanks to Mr Satyendra Pandey and Mr Partha Pratim Gogoi, fellow labmates who have helped me with my queries at various stages of this project.

I would also like to offer my sincere thanks to Dr Suhas Ettammal, my expert supervisor, for his insightful suggestions on my project and for guiding me towards various opportunities.

My family and friends, especially Sanjay Sriraj, Sandra Maria Jose and Reshma Thampy, have provided constant support throughout my project. I would like to express my gratitude towards them at this point.

I would also like to acknowledge the Infosys Foundation and DST for providing me with the necessary financial support to do this project. Finally, I would like to thank IISER Pune and IIT Bhubaneswar for providing the required infrastructure to carry out this project.

## Table of Contents.

1.	Introduction.	10
2.	Aerosols in the Earth Climate system: A literature review.	
2.1	What are aerosols?	11
2.2	Aerosol effect on radiation.	13
2.3	Challenges and motivation	15
2.4	Study Region	17
3.	Data.	
3.1	Moderate Resolution Imaging Spectroradiometer (MODIS)	18
3.2	Modern-Era Retrospective analysis for Research and Applications (MERRA)	20
3.3	Atmospheric InfraRed Sounder (AIRS)	20
3.4	Indian Meteorological Department (IMD)	20
4.	Materials and Methods.	
4.1	Preliminary data Quality Control and Screening	21
4.2	Temporal Correlation Analysis.	22
4.3	Regression Analysis.	22
4.4	Sensitivity Analysis.	23
4.5	Night time Analysis.	24
5.	Results and discussion.	
5.1	Spatial and temporal trends in AOD	24
5.2	Spatial and temporal trends in Tmax and Tmin	27
5.3	Spatial and temporal trends in cloud fraction	30
5.4	Spatial and temporal trends in total column water vapour	32
5.5	Spatial and temporal trends in Angstrom exponent	33
5.6	Correlation analysis.	

5.6.1	Preliminary correlation analysis.	<b>35</b>
5.6.2	AOD - Tmax correlation after accounting for CFR	<b>36</b>
5.6.3	AOD - Tmax correlation after accounting for CFR & TWV	<b>37</b>
5.7	Regression analysis.	<b>37</b>
5.7.1	Spatial patterns in aerosol effect for different seasons.	<b>38</b>
5.7.1.1	DJF (Winter)	<b>39</b>
5.7.1.2	MAM (Pre-monsoon)	<b>40</b>
5.7.1.3	SON (Post monsoon)	<b>41</b>
5.7.2	Comparison between MERRA and MODIS results.	<b>41</b>
5.8	Sensitivity analysis.	
5.8.1	Aerosol Optical Depth	<b>43</b>
5.8.2	Angstrom Exponent	<b>44</b>
5.8.3	Maximum Temperature	<b>45</b>
5.9	Night time analysis.	<b>46</b>
5.10	Daytime, nighttime and net daily aerosol direct effect.	<b>47</b>
5.11	Effects on the diurnal temperature range (DTR)	<b>49</b>
6.	Summary and Conclusions	<b>50</b>
	References	<b>52</b>

## List of figures.

2.1. Annual mean MODIS aerosol optical depth (2001-10) at 550 nm.....	12
2.2. Direct effect and the first indirect effect (cloud albedo effect).....	13
2.3. Comparative strength of different radiative forcings.....	15
2.4. Annual AOD climatology (2002 - 19) from MODIS (550 nm) .....	17
4.1. Study regions. ....	23
5.1. Spatial trends in AOD, 550 nm (a) MODIS b) MERRA .....	25
5.2. Spatial distribution of AOD (MODIS, 550 nm) during (a)DJF (b)MAM (c)SON ...	26
5.3. Spatial distribution of AOD (MERRA, 550 nm) during (a)DJF (b)MAM (c)SON ...	27
5.4. Spatial distribution of surface air temperature (a) Tmax (b) Tmin.....	28
5.5. Spatial distribution of Tmax during (a) DJF (b) MAM (c) SON.....	29
5.6. Spatial distribution of Tmin during (a) DJF (b) MAM (c) SON.....	29
5.7. Spatial distribution of CFR during (a) daytime (b) nighttime .....	30
5.8. Spatial distribution of daytime CFR during (a) DJF (b) MAM (c) SON.....	31
5.9. Spatial distribution of nighttime CFR during (a) DJF (b) MAM (c) SON .....	31
5.10. Spatial distribution of TWV vapour during (a) Daytime (b) Nighttime .....	32
5.11. Spatial distribution of daytime TWV during (a) DJF (b) MAM (c) SON.....	33
5.12. Spatial distribution of daytime TWV during (a) DJF (b) MAM (c) SON.....	33
5.13. Spatial distribution of MODIS AE.....	34
5.14. Spatial distribution of AE during (a) DJF (b) MAM (c) SON .....	34
5.15. Correlation between AOD and Tmax (a) DJF (b) MAM (c) SON.....	35
5.16. Correlation between AOD and Tmax when changes in cloud fraction are accounted for during (a) DJF (b) MAM (c) SON .....	36
5.17. Correlation between AOD and Tmax when changes in cloud fraction and water vapour are accounted for during (a) DJF (b) MAM (c) SON.....	37
5.18. $\Delta$ AOD vs $\Delta$ Tmax,over NI - NW.DJF, 2002-19.....	38
5.19. The spatial distribution of daytime aerosol effect. (a) MODIS, DJF (b) MODIS, MAM (c) MODIS SON (d) MERRA, DJF (e) MERRA, MAM (f) MERRA, SON.....	39
5.20. Potential mechanism as to how scattering aerosols cool the surface while absorbing aerosols warm the surface.....	40

5.21. Region-wise aerosol effect (a) MODIS, slope (b) MERRA, slope (c) MODIS, actual temperature change (d) MERRA actual temperature change.....	<b>42</b>
5.22. Sensitivity of aerosol effect ( $^{\circ}\text{C}/\text{unit AOD}$ ) to AOD (a) DJF (b) MAM (c) SON...	<b>43</b>
5.23. Sensitivity of aerosol effect ( $^{\circ}\text{C}/\text{unit AOD}$ ) to AE (a) DJF (b) MAM (c) SON.....	<b>44</b>
5.24. Sensitivity of aerosol effect ( $^{\circ}\text{C}/\text{unit AOD}$ ) to Tmax (a) DJF (b) MAM (c) SON.	<b>45</b>
5.25. The spatial distribution of nighttime aerosol effect (a) MODIS, DJF (b) MODIS, MAM (c) MODIS, SON (d) MERRA, DJF (e) MERRA, MAM (f) MERRA, SON .....	<b>46</b>
5.26. Region-wise aerosol effect (a) MODIS, daytime (b) MODIS, nighttime (c) MODIS, net temperature change (d) MERRA, daytime (e) MERRA, nighttime (f) MERRA, net temperature change.....	<b>48</b>
5.27. Region-wise aerosol associated DTR change (a) MODIS (b) MERRA.....	<b>49</b>



## **Abstract.**

Atmospheric aerosols are an essential component of Earth's climate system that interact with the radiation falling on Earth through direct, indirect and semi-direct effects. Multiple studies have explored the impact of aerosols on surface-reaching solar radiation. These studies have shown an overall negative radiative forcing globally. It is also well known that aerosol-induced radiation changes have a corresponding effect on surface air temperature, an essential parameter for meteorology and human life on the surface. However, not many studies have explored this issue on local or regional scales, especially using observational data due to the complex nature of this relationship which is influenced by land surface parameters in addition to short and longwave radiation. This study attempts to quantify the effect of aerosols on surface air temperature using long term satellite observations (2002-2019) over the Indian region on annual and seasonal time scales.

It is found that aerosols reduce the daytime surface temperature by as much as  $-1.0$  to  $-1.5$  °C/unit aerosol optical depth (AOD) during the winter season (Dec-Jan-Feb, DJF) and  $\sim -0.5$  to  $-1$  °C/unit AOD during the post-monsoon season (Sep-Oct-Nov, SON) over most of North India. A surprising observation was observed during March to May (MAM), where aerosols induced warming of  $\sim 0.03$  °C/unit AOD -  $0.97$  °C/unit AOD over Northern India. This warming signature's timing and spatial distribution point to the possibility of absorption by predominantly dust aerosols and the highly reflective nature (surface albedo) of land surface during this period to be the plausible causes.

A similar analysis for nighttime reveals an all seasons warming of  $\sim 1 - 2$  °C/unit AOD during DJF and SON while being in the range of  $2-3$  °C/unit AOD over most of India during MAM. The net daily aerosol effect is smaller during DJF and SON than MAM (significant positive aerosol effect) due to the similarity in signs of aerosol forcing during daytime and nighttime (overall addition). Overall, net daily aerosol effect is observed to be in the range of  $-0.2 - 0.4$  °C annually over different regions. Aerosols are also observed to reduce the diurnal temperature range (DTR) during all seasons. Annually,

the DTR varies around -0.7 to -0.4 °C. Northern India shows higher aerosol effect compared to Southern India. Similar results were obtained using MERRA reanalysis AOD dataset with the temperature having a slightly higher sensitivity to reanalysis AOD than that observed using satellite aerosol information (MODIS). Several sensitivity analyses by potentially varying aerosol loading, temperature and size are also discussed.

# Surface Temperature Changes due to Aerosols using Satellite Observations over India.

## 1 Introduction.

Since the advent of the industrial revolution in the 1850s, human civilization has been growing at an exponential rate. The rise of the human population and the need to sustain them have put an ever-growing burden on natural resources and the environmental balance of our Earth system. This has started a massive debate on the sustainability of human development and anthropogenic climate change.

Atmospheric aerosols are tiny particles suspended in the atmosphere that can be of both natural and anthropogenic origin. These particles have a small mass fraction but play a substantial role in Earth's climate through their interactions with radiation (both solar and terrestrial) and clouds. The mechanism of these processes and their complexities are still not fully understood. According to the 2014 IPCC report, aerosols and clouds contribute the most significantly to uncertainty in estimates and interpretations of the Earth's changing energy budget. Much work has thus been done to find the radiative effects of aerosols, which has led to considerable progress in decreasing the uncertainty in aerosol radiative forcing estimates.

Surface air temperature is an essential parameter for meteorology. It affects nearly all other weather aspects and human life in general. Any aerosol induced change in radiation is expected to affect the surface air temperature as well. However, few studies have tried to see how this change in radiative forcing affects the surface temperature using observations. This is because the inherent complexity of the different mechanisms influencing surface temperature makes modelling studies more feasible for such studies. The lack of high-quality data also limited earlier studies done using

observations. However, the availability of high-quality satellite datasets from the early 2000s onwards allows the community to explore these problems.

This study aims to understand better how radiative changes due to aerosols affect the surface air temperature using satellite observations with two primary objectives.

1. Establish a simple and effective method for calculating the surface air temperature change due to aerosols while accounting for confounding variables. This would effectively help us answer what factors affect the aerosol temperature relationship and the surface temperature change for a given aerosol loading.
2. Understand the spatial and temporal patterns in the observed relationships, if any.

## **2 Aerosols in the Earth Climate System: A Literature review.**

### **2.1 What are aerosols?**

Aerosols are tiny particles suspended in the atmosphere that are significant components of Earth's radiation budget. Aerosols can be natural like dust, sea salt or anthropogenic like carbonaceous aerosols (black carbon, organic carbon), sulphates, nitrates etc. Combustion processes and biomass burning are major sources of carbonaceous aerosols, but natural processes like forest fires also emit significant carbonaceous aerosols into the atmosphere. Likewise, large amounts of sulphate aerosols are also emitted into the atmosphere from natural sources like volcanoes and marine phytoplankton. Anthropogenic activities like fossil fuel burning also emit volatile organic compounds into the atmosphere, which can later condense to form secondary aerosols. Figure 1.1 provides an overview of the various types of aerosols predominant in different parts of the world.

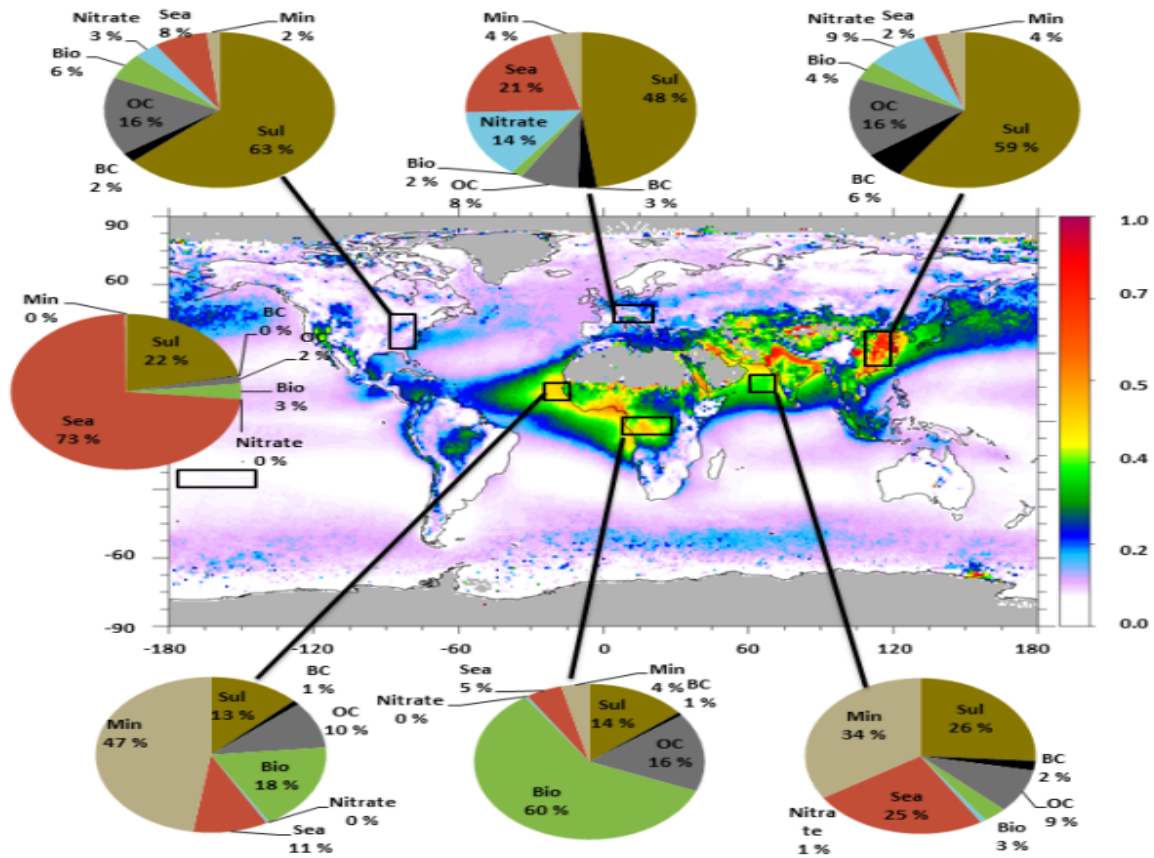


Fig 2.1: Annual mean MODIS aerosol optical depth (2001-10) at 550 nm. The pie charts show the contribution of different aerosol types in the total AOD in the regions as estimated by a global aerosol model (Myhre *et al.*, 2009). Aerosol types are Sul (sulphate), BC and OC from fossil fuel usage, Bio (OC and BC from biomass burning), Nitrate, Sea (sea salt), and Min (mineral dust). Grey areas indicate a lack of MODIS data. Adapted from Myhre *et al.* 2013.

Aerosols can be classified into different groups depending on their origin (continental and marine), formation mechanism (primary and secondary) and interaction with radiation (absorbing and scattering). Aerosols in the troposphere have a short residence time of about one day to two weeks, while aerosols in the stratosphere can have residence times of up to a year. Once in the atmosphere, the size and chemical composition of the aerosols may change through chemical reactions, condensation or

uptake of water (hygroscopicity). Aerosols depending on their chemical composition, source of formation, particle and size distribution, can have varying effects on the climate.

## 2.2 Aerosol effects on radiation.

A significant amount of work has been carried out to explore the various effects of aerosols on the Earth system, primarily how it affects the surface radiation, which is quoted usually as net aerosol forcing ( $Wm^{-2}$ ). Aerosols affect the climate through direct, semi-direct and indirect effects. Aerosols scatter or absorb radiation depending on their size, type (whether absorbing or scattering) and composition, affecting the amount of radiation falling on the surface. This is called the direct effect of aerosols (Fig 2.2.a), as the aerosols interact directly with the radiation in this method (Kiehl and Briegleb, 1993; Haywood and Shine, 1995).

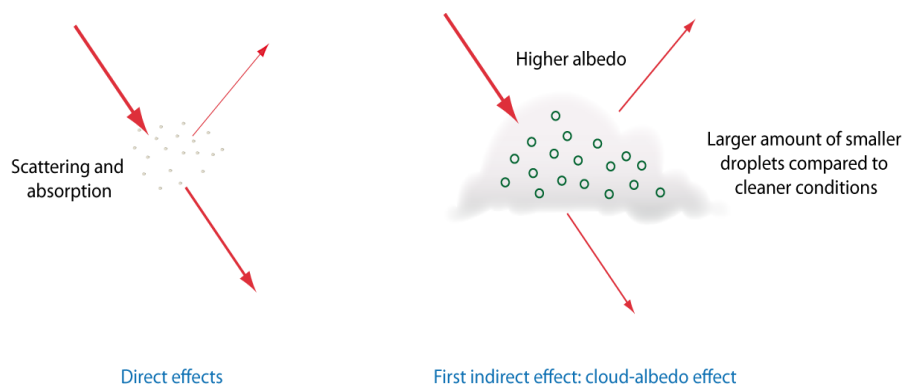


Fig 2.2: Direct effect and the first indirect effect (cloud albedo effect). The second albedo effect and semi-direct effect are not represented. Adapted from [http://www.climate.be/textbook/chapter4\\_node3\\_2.html](http://www.climate.be/textbook/chapter4_node3_2.html)

Aerosols can also act as cloud condensation nuclei (CCN) and ice nuclei (IN). The increase in aerosol number density with constant water content and cloud height increases the optical depth and the cloud's albedo. This reduces the amount of radiation falling on the surface. This effect was first pointed out by Twomey (1974). This would

be described as the first indirect effect of aerosols (Fig 2.2). The smaller droplet sizes would also imply longer residence times for the clouds suggesting a prolonged effect on the radiative balance. This is called the second indirect effect or cloud lifetime effect of aerosols. (Albrecht, 1989)

Absorbing aerosols in elevated layers of the atmosphere can also change the vertical temperature profile, thereby affecting the upward convection and formation of clouds. The absorbing aerosols can also facilitate the evaporation of existing clouds, thereby affecting the radiative balance. This is a semi-direct method as the aerosols themselves do not interact with the radiation directly and do not form CCNs or INs as in indirect effect (Hansen et al. 1997).

Kiehl and Briegleb (1993) tried to quantify the direct effect of sulphate aerosols on the radiation falling on the surface in one of the first attempts to do so. They found that sulphate aerosols cool the surface of the earth by  $-0.3 \text{ Wm}^{-2}$  annually. Another study by Haywood and Shine (1995) found the direct effect of soot and black carbon on surface temperature to be in the range of  $+0.03 \text{ Wm}^{-2}$  to  $0.24 \text{ Wm}^{-2}$ , comparable to the direct effect of sulphate aerosols found by Kiehl and Briegleb. The current estimates of composite aerosol direct effect from the IPCC, 2014 report stands at  $-0.45 \pm 0.5 \text{ Wm}^{-2}$ .

A modelling study by Jones et al. (1994) found the indirect forcing due to anthropogenic sulphate aerosols to be  $-1.26 \text{ Wm}^{-2}$  annually in one of the earliest attempts to quantify the indirect forcing due to aerosols. But this study doesn't take cloud lifetimes into account. Also aerosol species other than sulphates can become CCNs. Thus the indirect effect could be more significant than the above figure. Aerosols, along with clouds, contribute the most significant uncertainty to estimates and interpretations of the Earth's changing energy budget (IPCC report, 2014). Most of this uncertainty comes from the estimation of the indirect effect. Similar studies predict the range of the indirect effect to be between  $-1.1$  to  $-3.7 \text{ Wm}^{-2}$  (IPCC report, 2001), while later reports (IPCC report, 2014) put it between  $\sim -0.4$  to  $-2.6 \text{ Wm}^{-2}$  with a median of  $-1.4 \text{ Wm}^{-2}$ . Note that

the median value is more than three times the best estimate of direct effect. Overall, the direct effect has a smaller uncertainty associated with it compared to the indirect effect.

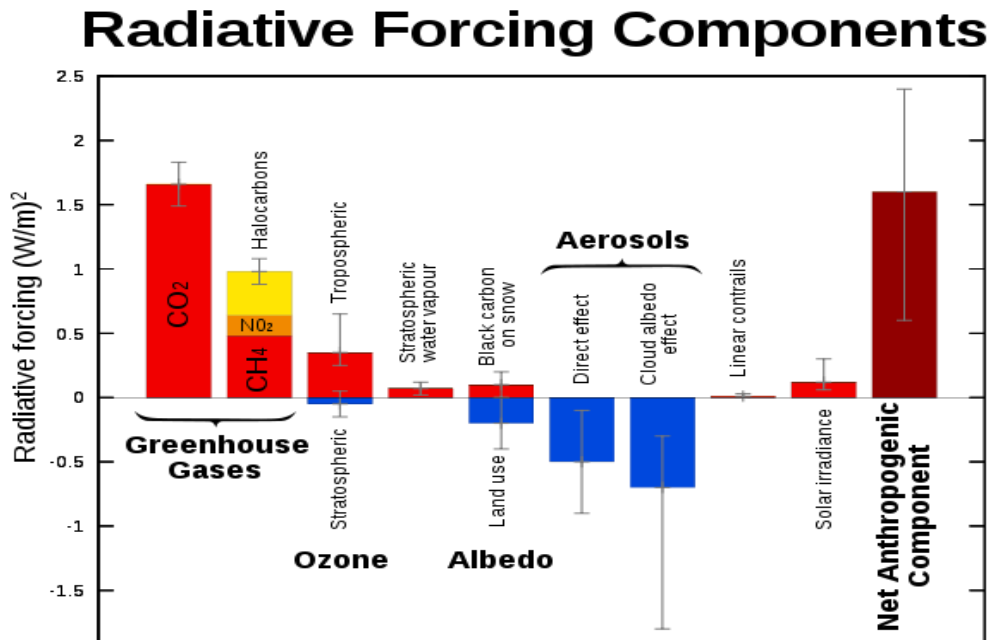


Fig 2.3: Comparative strength of different radiative forcings. Adapted from [https://energyeducation.ca/encyclopedia/Radiative\\_forcing](https://energyeducation.ca/encyclopedia/Radiative_forcing)

In comparison, the greenhouse gases exert a net radiative forcing of  $\sim 2.6 \text{ Wm}^{-2}$ . The radiative forcing due to aerosols could thus potentially offset the net positive forcing due to other components if we were to believe the highest estimate of cooling due to aerosols from both methods. Ramanathan and Feng (2009) have found that aerosols mask as much as 47% of the global warming effect. The sign of the semi-direct effect varies depending on the location of the aerosols with respect to the clouds (Koch and Del Genio., 2010). Thus, understanding aerosols' effects on radiation and other meteorological parameters is crucial in determining their effects on weather, climate, and changes in them.



### **2.3 Challenges and motivation.**

As we can see from the previous section, there is a consensus that there is a negative forcing due to aerosols at the surface. Surface air temperature is an important parameter for meteorology and human life in general. Air temperature affects nearly all the weather parameters like the rate of evaporation, relative humidity, pressure and precipitation patterns. Surface air temperature is measured at the height of 2m above the surface of the earth. Changes in radiation induced by aerosols are expected to have their corresponding effect on surface air temperature. However, not many studies have explored this change in radiative forcing and its impact on surface temperature using observations.

The aerosol distribution shows large spatiotemporal variation in terms of the type and loading. Aerosol forcing is generally quoted in terms of net annual forcing. Seeing how aerosols type and loading can change within a year and regionally is vital to understand short time scale effects of aerosols. Thus, it is relevant to see how aerosols affect the surface temperature seasonally on regional scales.

In the studies done over the Indian region, Krishnan and Ramanathan (2002) found that absorbing aerosols while heating the atmosphere reduced the temperature at the surface while pointing towards the possibility of warming in regions non-local to the aerosol haze to balance local cooling. Roy (2008) found the effect of aerosols on surface air temperature over India through linear regression. However, they were limited by the amount of data available to them (5 years). This study also doesn't take the seasonalities of aerosols and surface air temperature into account. Meehl et al.(2007) found that black carbon (an absorbing aerosol) enhanced the lower tropospheric heating while reducing the amount of radiation falling on the surface thereby affecting the monsoon over the region. Absorbing aerosols like dust are also reported to exacerbate heat waves by enhancing the surface air temperature (Dave et al., 2020). It is also expected that aerosols would affect the surface energy balance and moist heat stress by modulating surface air temperature. Thus understanding the interaction

between the two is critical for meteorology, climate and human life on the planet's surface.

These studies were also limited by the lack of long term observations and the inherent complexity of the aerosol climate interactions, which made modelling studies more feasible for such studies. However, the availability of high-quality space-borne measurements of aerosol properties and other climate variables, especially from early 2000s onwards, allow us to quantify aerosols' effect on surface temperature. Thus, the study is an effort to quantify the all-season effect of aerosols on the surface temperature over the Indian region.

## 2.4 Study Region

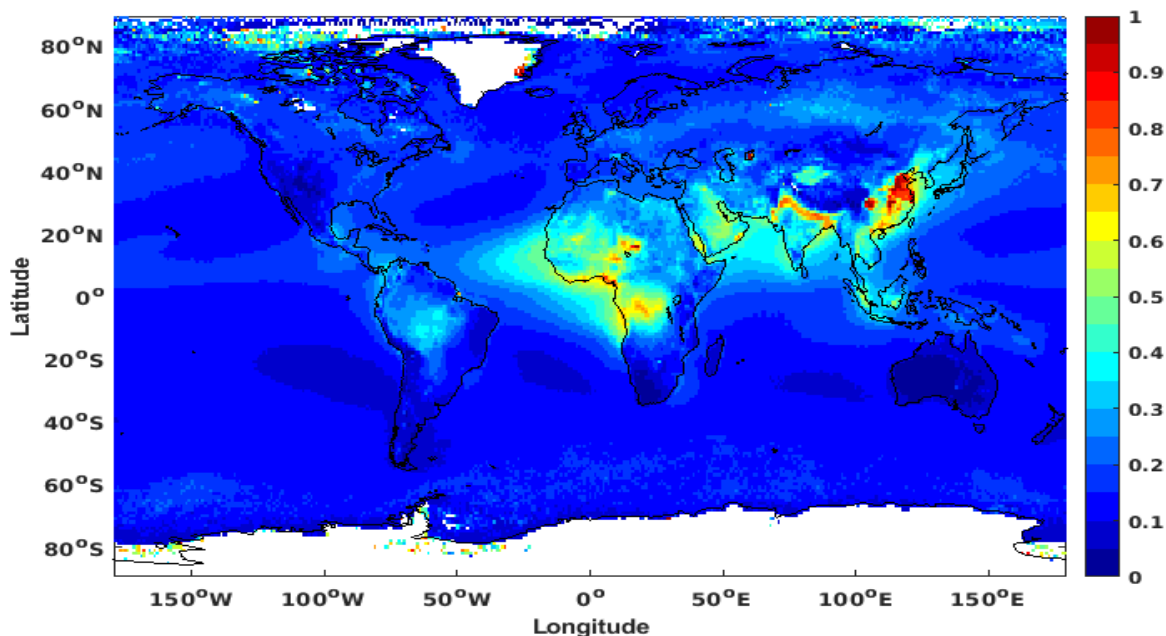


Fig 2.4: The annual mean aerosol optical depth climatology (2002 to 2019) from MODIS at 550 nm.

Fig.2.4. shows the annual mean climatology of aerosol loading observed globally using the MODIS (Terra) for 2002 to 2019. India, along with China and Western Africa, forms major regions with high aerosol loading. These regions are all impacted by different

aerosol types. For example, over Africa, desert dust and biomass burning dominate the loading. In contrast, over India, anthropogenic activities coupled with the high dust emissions from the Thar desert dominate the aerosol composition. Over China, similar natural and anthropogenic aerosols emissions dominate the overall loading. For our work, we choose the Indian region for our analysis due to the following reasons,

1. India, especially Northern India, has one of the world's highest population density and numerous industries that emit aerosols to the atmosphere (Sarkar et al., 2005). The high loading conditions make it one of the most polluted or aerosol laden regions in the world.
2. This region is also heavily affected by desert dust emissions from the Great Indian Desert "Thar" and the arid areas to the subcontinent's North-Western areas (Dey et al., 2010; Singh, 2014). The South Asian monsoon is also characterised by the large transport of sea-salt aerosols over to the landmass from the Arabian Sea region. The interaction between natural dust and anthropogenic emissions makes India an excellent natural laboratory to study their potential mixing, modification to optical properties and its effect on climate.

### **3 Data.**

The aerosol optical depth (AOD), cloud fraction (CFR) and total water vapour (TWV) data used in this study were obtained from the NASA Giovanni archive (<https://giovanni.gsfc.nasa.gov/giovanni/>) for the period from 2002 September to 2019 December. All the variables are at a spatial resolution of  $1^\circ \times 1^\circ$  at daily temporal resolutions.

#### **3.1 Moderate Resolution Imaging Spectroradiometer (MODIS)**

Aerosol optical depth (AOD) is a dimensionless quantity and measures integrated column extinction of direct solar radiation. Thus, it is an excellent quantifiable proxy for the aerosol loading in the atmosphere. The Moderate Resolution Imaging

Spectroradiometer (MODIS) is a multispectral imaging radiometer onboard the NASA's Terra and Aqua satellites that provide global high-quality daily observations of the earth in a wide spectral range (0.4 $\mu$ m to 14.4 $\mu$ m in 36 bands) at varying spatial resolutions (250m,500m and 1km). AOD is retrieved using the Deep Blue (over land, Hsu et al .2013) and Dark Target Algorithms (over the ocean and vegetated/dark soiled land, Levy et al., 2013). The combined Dark Target and Deep Blue AOD at 550nm (MOD08\_D3 v6.1) is used for the present study, which combines both the Dark Target and Deep Blue algorithms based on the surface NDVI (Normalized Difference Vegetation Index). Mhawish et al. (2017) have shown that the combined product performs better than individual dark target and deep blue algorithms and is applicable over a larger area over the Indian region.

The MODIS Terra/Aqua aerosol products are of high accuracy and are validated by multiple studies over the land and oceanic regions around India (e.g. Vinoj et al., 2004, 2010, Mhawish et al., 2017). The retrieval algorithms are updated periodically (Remer et al., 2005) to improve the accuracy. The MODIS AOD is typically reported in the following wavelengths: 0.47, 0.55, and 0.65  $\mu$ m with an error of  $\pm 0.05 \pm 15\% \tau$  (Kaufman and Tanré, 1998). In this study, only AOD at 0.55  $\mu$ m is used. In addition, the latest collection (collection 6) (Platnick et al., 2017) with significantly reduced uncertainty is used. Observations from MODIS are widely used for aerosol and air quality research (Babu et al., 2013; Gupta et al., 2006, 2013; Vinoj and Pandey, 2016; Pandey et al., 2017; Rupakheti et al., 2019).

Angstrom exponent (AE), a simple representation of aerosol size, is also obtained from MODIS. The Angstrom exponent is given by

$$\alpha = - \log (\tau_1/\tau_2)/\log(\lambda_1/\lambda_2),$$

Where  $\tau_1$  and  $\tau_2$  are the optical depths at wavelengths  $\lambda_1$  and  $\lambda_2$ , respectively. The AE is calculated using 412 nm and 470 nm as reference wavelengths. AE is a measure of the size of the aerosol particles. Coarser, larger (mostly natural) particles have a smaller AE, while smaller particles (mostly anthropogenic) have a larger AE.

### **3.2 Modern-Era Retrospective analysis for Research and Applications (MERRA)**

The Second Modern Era Retrospective Analysis for Research and Applications (MERRA-2) AOD data is a long term global reanalysis product starting from 1980. It is the first reanalysis dataset to assimilate the aerosol interactions with other climate processes. It assimilates data from a variety of products like the Advanced Very High Resolution Radiometer (AVHRR; 1979-2002), MODIS (Terra (2000~present) and Aqua (2002~present)), Multiangle Imaging Spectrum Radiometer (MISR;2000~2014) and AERONET (1999~2014) (Molod et al.,2015; Gelaro et al.,2017). It is based on a version of the GEOS-5 atmospheric data assimilation system. Comparisons between 15 years of daily aerosol optical depth from MERRA-2 and ground-based AERONET observations show a high degree of consistency (Gueymard and Yang, 2020).

The data was obtained in  $0.625^\circ \times 0.5^\circ$ , but the data was regridded to  $1^\circ \times 1^\circ$  grids to make it consistent with other datasets. The product was used to provide further validation to the results obtained using MODIS products.

### **3.3 Atmospheric InfraRed Sounder (AIRS)**

Atmospheric Infrared Sounder (AIRS) onboard NASA's Aqua satellite is a hyperspectral atmospheric sounder with 2378 infrared channels and four visible/near-infrared channels, which provides daily long term global observations of land, ocean and atmosphere (Pagano et al. 2006; Chahine et al. 2006). Cloud fraction (CFR) is a dimensionless quantity describing the fraction of a pixel under cloud cover. Total column water vapour (TWV) amount of water vapour in the atmosphere column in  $\text{kg/m}^2$ . The level 3 daily products (AIRSX3STD V007) of both CFR and TWV were used in this study (Tian et al. 2020), the latest version of the datasets. Validation studies show good agreement between AIRS data and radiosonde data within mission specified accuracy bounds (Prasad and Singh., 2009; Kahn et al., 2008; Milstein and Blackwell. 2015).

### **3.4 Indian Meteorological Department (IMD)**

The Indian Meteorological Department (IMD) provides daily gridded data ( $1^{\circ}\times 1^{\circ}$ ) for maximum surface air temperature (Tmax) and minimum surface temperature (Tmin). A modified form of Shephard's angular weighting algorithm is used, which interpolates station data from 395 stations all over India (Rajeevan et al., 2009). The root mean squared error (RMSE) is observed to be less than  $0.5^{\circ}\text{C}$  for almost all parts of the country. The data set has been widely used in studies of heatwaves, cold waves, and numerous environmental applications. (eg. Naveena et al., 2021; Rohini et al., 2016; Srivastava et al., 2017).

## **4 Methods**

### **4.1 Preliminary data quality control and screening**

Several issues need to be addressed before using satellite aerosol datasets for detailed analysis. The satellites may sometimes mistake small clouds for aerosols during the retrieval due to sub-grid cloud contamination though the major portion of the grid may be cloud-free. The optical depth could thus be reported as high in these cases. Sometimes, the radiance from the surrounding cloudy pixels may leak into the current pixel resulting in adjacency effects. The adjacency effect lowers the AOD leading to a bias which affects lower AOD values more. Therefore, the data were screened for outliers by removing the highest and lowest 5th percentiles of data for a grid point. It may be mentioned that MODIS retrieval uses one of the best cloud screening methods and its retrieval is considered the best available to the community. The above screening is done only to be confident twice to the extent possible. The mountainous regions were avoided to avoid the altitudinal dependence of AOD and temperature. The coarse resolution of the data may unnecessarily lead to false correlations or relationships due to largely varying altitude and hence surface temperatures. The regions where the average height above sea level exceeded 500m were thus not considered for the analysis. This first level of screening altogether avoids any issues related to clouds or topography related issues.

In addition, all meteorological variables are also affected by seasonality and long term trends. Similar seasonality and long term trends in different parameters may induce false correlations. Therefore, it is vital that we use residuals for the study rather than the variables themselves. Residuals at each time point were thus calculated by removing the weekly mean (calculated using a seven-day running window centred at the data point) from the data point to remove the seasonality related correlations. The monsoon season (JJA, June-July-Aug) was avoided from the analysis to prevent the effect of rainfall on the surface air temperature-aerosol relationship.

#### **4.2 Temporal Correlation Analysis**

The first objective was to identify if there is any discernible relationship between the aerosol and surface temperature distributions. For this purpose, the correlation between deseasonalized, detrended AOD and Tmax were calculated. The significance of the correlation coefficient was found through the t-test. Next, the role of other variables (cloud fraction and total column water vapour) were established by doing a partial correlation analysis between AOD and Tmax while accounting for changes in the other two variables.

#### **4.3 Regression analysis**

Northern India has one the highest aerosol loading in the world. Hence, the region was considered a preliminary study region (Fig 4.1.a) to observe the effect of aerosols on surface air temperature. The influence of clouds and water vapour on aerosol surface air temperature is assumed to be lesser during winter due to clear skies and dry conditions with low column water vapour content. The residuals of AOD, CFR and TWV were regressed on Tmax using multiple linear regression for the winter (DJF) season over the region. The slope of the aerosol term, in this case, would represent the effect of a unit change in AOD on surface temperature.

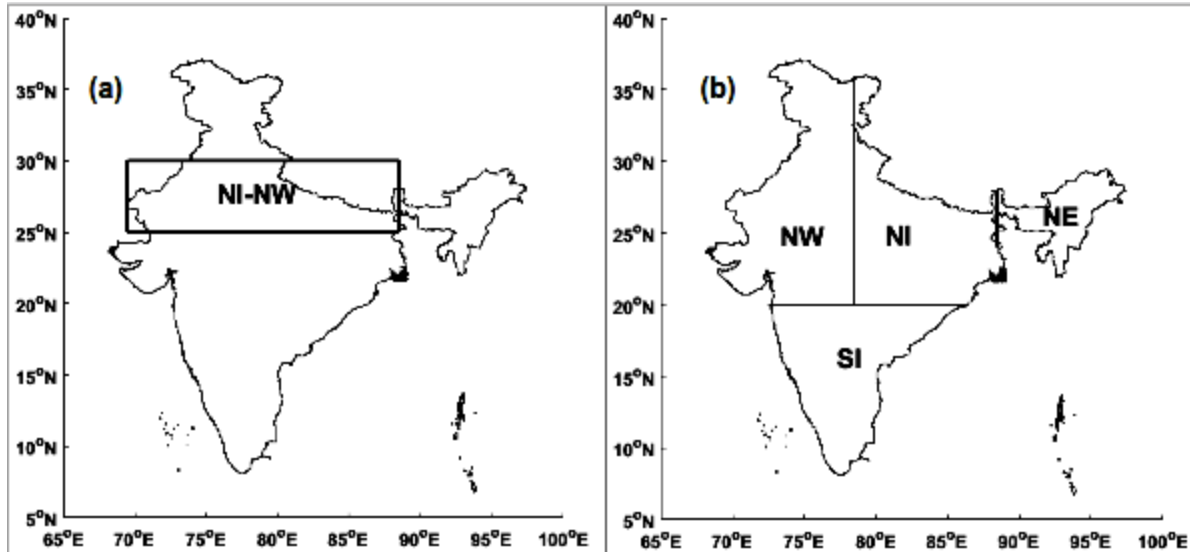


Fig 4.1: Study regions. (a) Preliminary region (NI-NW) selected for regression analysis. (b) Sub-regions selected within the study area to study the spatial nature of aerosol - surface air temperature interactions. Here, NI- North India; NW- North-West India; NE- North-East India; SI - South India.

However, aerosol properties vary considerably, both spatially and temporally. Hence, the same analysis was conducted separately at each gridpoint for all the seasons, allowing us to discern any spatial patterns in the aerosol-surface air temperature (AOD-Tmax) relationship. The analysis was then conducted for different seasons and then averaged over the different regions in India (Fig 4.1.b) to estimate the regional effects of aerosols on Tmax. Finally, the statistical significance of the results was calculated using a simple t-test.

#### 4.4 Sensitivity Analysis

A similar analysis was repeated using MERRA-2 AOD data to confirm if the patterns seen could be replicated using a reanalysis dataset. The sensitivity of the observed aerosol effect to changes in AOD, Tmax, and AE was also explored. For example, if the sensitivity of aerosol effect to changes in aerosol loading were to be calculated, the AOD data at a grid point was divided into bins of 25 percentile each. The regression analysis was done using data corresponding only to points in the same bin. Regional



averages of aerosol effect in a particular bin were then calculated and plotted vs the percentile of variables considered. If there were no relationship, all plots would show a slope equalling zero. However, any dependence will be observed as a non-zero slope.

#### **4.5 Night time analysis.**

Aerosols primarily interact with short wave radiation during the daytime. During night time, the Earth and the atmosphere both release back the heat absorbed during day time as longwave radiation and aerosols interact with these radiation or themselves release longwave radiation. Thus, studying the aerosol-surface air temperature during daytime and night time allows us to see these differences and estimate the overall daily effect of aerosols. However, an analysis as done for daytime is challenging for the nighttime due to the absence of AOD data. Here, we assume that AOD during daytime remains the same during nighttime and carry out a similar analysis. This is a first cut assumption and needs to be explored further. However, it has to be noted that such studies are lacking to date.

Thus the regression and subsequent analysis were also conducted using residuals of AOD (daytime) and other parameters measured during the night. These parameters were nighttime CFR, TWV and Tmin. The diurnal temperature range (DTR) is the difference between the maximum and minimum temperatures during a day. The influence of aerosols on DTR was also studied. The net aerosol effect on temperature could thus be calculated as the sum of aerosol effect during daytime and night time.

## 5 Results and Discussions.

### 5.1 Trends in AOD.

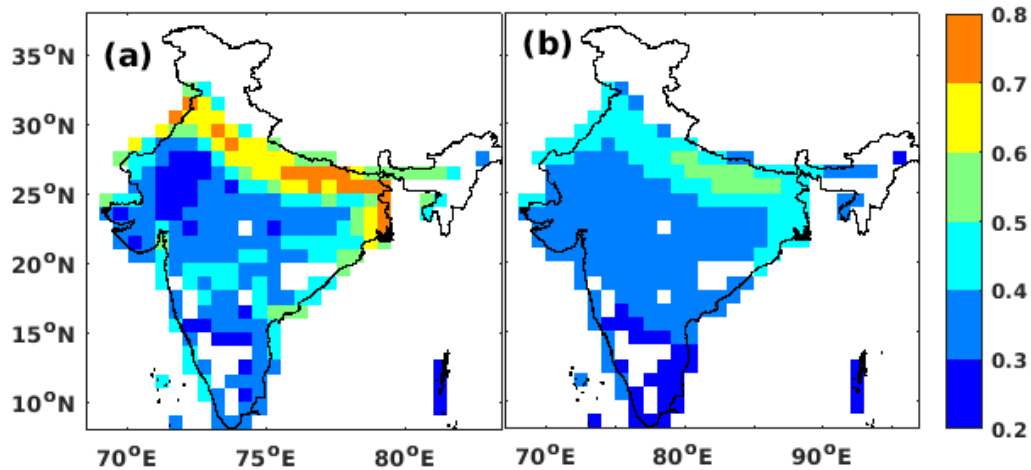


Fig 5.1: Spatial trends in Aerosol Optical Depth, 550 nm (a) MODIS b) MERRA.

The average annual MODIS AOD over the North Indian region is 0.51, which is 16% higher than the national average of 0.44 (2002 - 2019, see Fig. 5.1). One can observe higher aerosol loading, especially in the Indo Gangetic Plain (IGB) region in the range of 0.6 to 0.8. This could be due to the large population density along with the presence of a large number of industries. Central India shows moderate AOD values. Southern India shows relatively lesser AOD compared to other areas. The AOD shows a spatial gradient going from north to south.

The MERRA AOD shows relatively lower values compared to the MODIS AOD. Optical depth is seen to differ by  $\sim 0.1$  or more in regions of high aerosol loading. The spatial trends in AOD, however, remain consistent with those seen in MODIS.

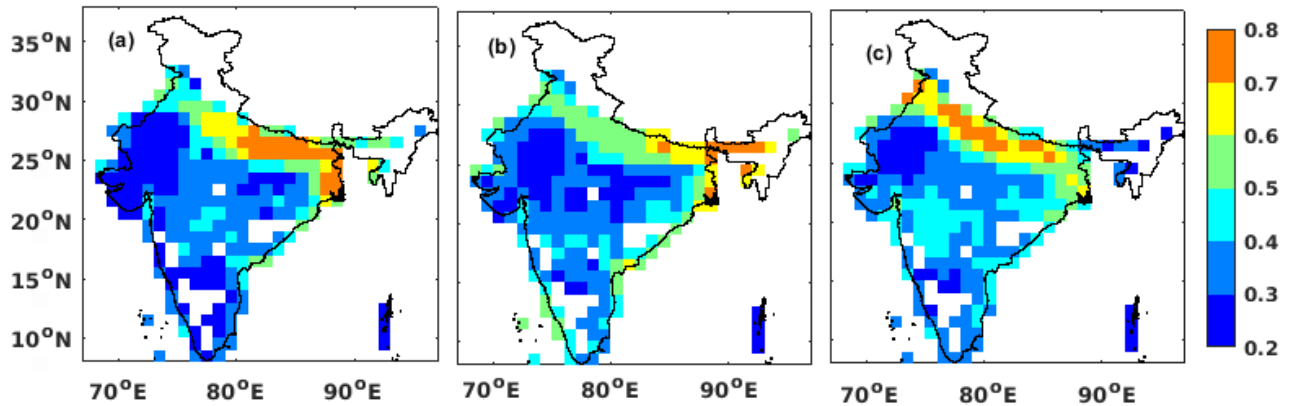


Fig 5.2: Spatial distribution of AOD (MODIS, 550 nm) during (a) DJF (b) MAM (c) SON.

The AOD (MODIS and MERRA) over most regions shows an increasing seasonality from DJF to JJA (maximum) and then decreases during SON. The high AOD over northern India (0.52) during the winter season (Fig:5.2.a, Fig:5.3.a) could be due to increased energy usage and the lower surface temperature, which implies a stable atmosphere and less dispersal of the accumulated aerosols (Srivastava et al., 2012). This leads to an accumulation of anthropogenic aerosols in the atmosphere which increases the AOD.

We see a slight decrease in AOD over many regions by as much as 0.1 during MAM. It may be noted that AOD is a column measure. Hence, changes in its magnitude indicate a composite change occurring throughout the column of the atmosphere. Therefore, the winter high and summer low could be a reflection of better dispersion throughout the column during summer and reduced dispersion/stagnant condition during winter. Northern India is influenced by dust particles transported from the adjacent Thar desert and the Arabian and Sahara desert, increasing the AOD during the MAM and JJA seasons (Deepshikha et al., 2006). In addition, vast lands of Northern India are arable. During the summer season, these exposed lands may enable the emission of fine dust particles into the atmosphere, which can further increase the AOD over the region. The AOD becomes maximum during JJA when the dust buildup is maximum

The south Asian monsoon scavenges a lot of the particulates in the atmosphere. Besides, higher relative humidity during SON and DJF means the AOD could increase due to increased particle size due to hygroscopic growth (Shaeb, 2019). The North Indian region is also affected by biomass burning (which happens mainly in November or MAM), increasing the average AOD in the area (Singh and Kaskoutis, 2014).

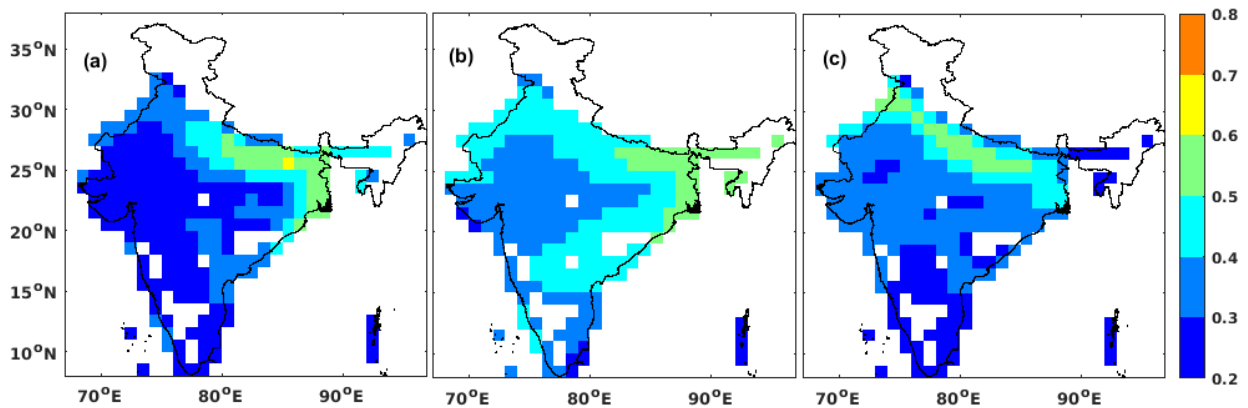


Fig 5.3: Spatial distribution of AOD (MERRA, 550 nm) during (a) DJF (b) MAM (c) SON.

As in the annual case, the AOD during different seasons differs in some regions for the two datasets by about 0.1 or more. But, the MERRA AOD shows the same spatial distribution as the MODIS AOD for all seasons (Fig 5.2 and 5.3). It is not surprising that MERRA is well capturing the AOD spatial distribution, as MERRA assimilates satellite AOD retrievals within its reanalysis system. The bias may result from an error in some other parameter or suppression of it to enable minimal overall error in the simulated climate.

## 5.2 Trends in Tmax and Tmin

In Fig. 5.4, The annual Tmax is highest over the north-west, central India, and the eastern coast (33-35°C). The presence of the Thar desert to the North West and the Deccan plateau in central to Eastern India could be the reason for higher Tmax in these regions. The western coast is seen to have a lower annual Tmax compared to the east by about 1-2°C. The western ghats have higher elevation (and vegetation) above the sea compared to the eastern ghats. This could be the reason for the difference in temperature between the two regions. Northern India shows moderately high annual Tmax. One can also see that regions with high aerosol loading show lesser maximum temperature compared to the surrounding regions. Although part of this could be attributed to the region's geography, this is another indication that aerosols may impact the surface air temperature.

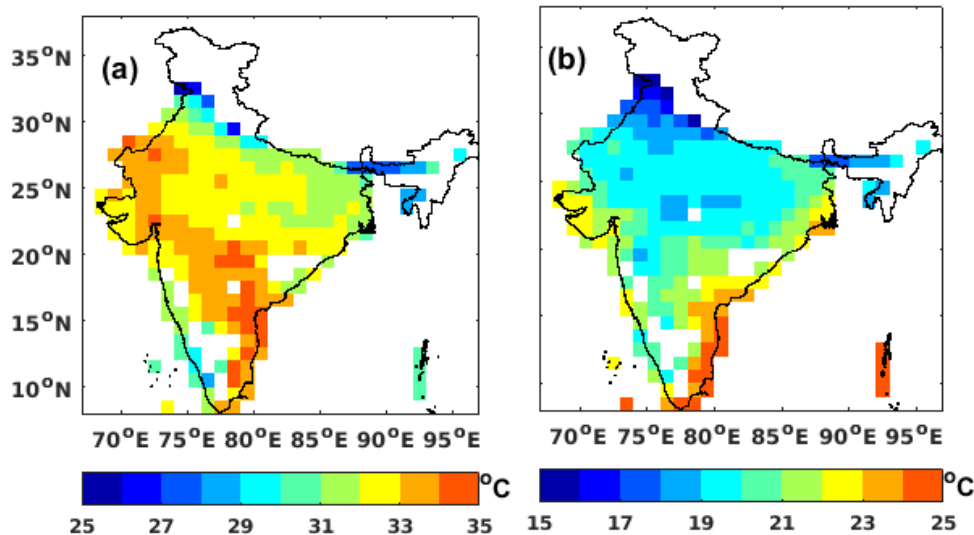


Fig 5.4: Spatial distribution of surface air temperature (2002-19)  
(a) Maximum temperature (Tmax) (b) Minimum temperature (Tmin).

The annual Tmin is seen to be highest over the eastern coast. The regions to the interior are seen to experience lower Tmin compared to regions closer to the coast. The variation between the two can be as much as 4-5°C.

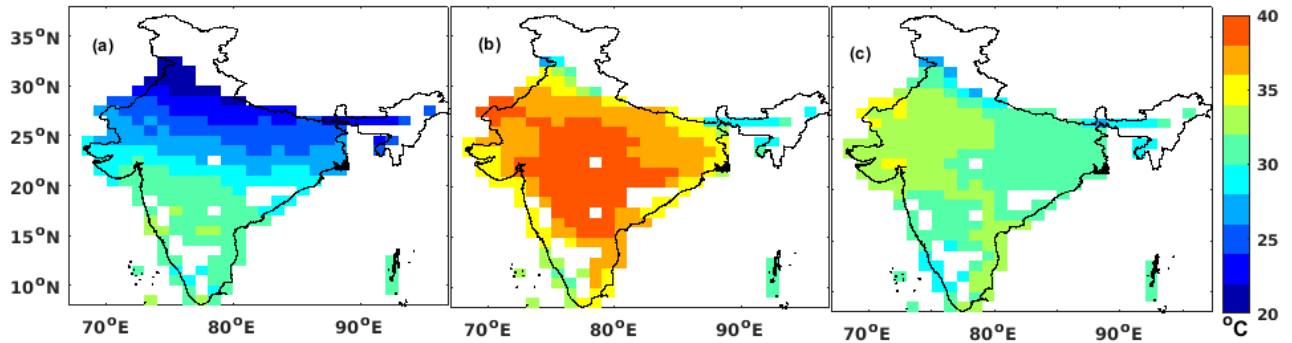


Fig 5.5: Spatial distribution of maximum temperature (Tmax) during (a) DJF (b) MAM (c) SON. The IMD Tmax temperature is averaged for each season for each grid point.

The surface air temperature also shows a distinct seasonality. The winter (DJF) season is marked by low temperatures throughout India. Tmax is moderately low (25-30 °C) in southern India while it can go below 10 °C over certain regions in North India. The temperature over India rises during the pre-monsoon (MAM) season. High temperatures are reported over central India and the Deccan Plateau during this season which can mostly be attributed to the terrain. The temperatures over some regions northwest and north India can be more than 45 °C. During SON, the temperatures over most of India are decreasing with average temperatures of 28- 34 °C over most places. Some regions may get rain from the retreating monsoon, which lowers the temperature, and this season generally marks a transition from the wet period to the dry season.

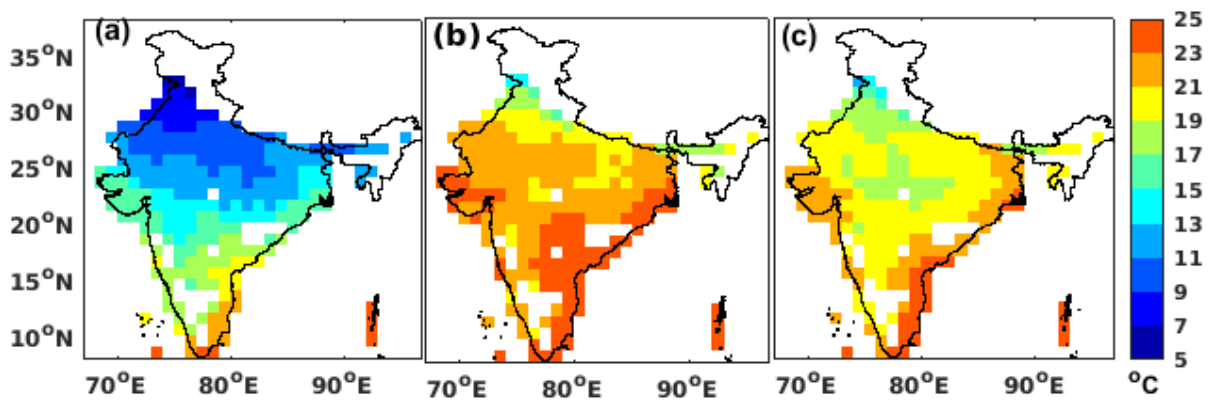


Fig 5.6: Spatial distribution of minimum surface air temperature (2002-19) (a) DJF (b) MAM (c) SON.

Tmin (see Fig. 5.6) shows similar seasonal and spatial trends as Tmax. Minimum temperatures are the lowest during DJF and could go below 0°C over some regions in the north. Tmin becomes maximum during MAM and then decreases to the values seen in SON. The eastern coast shows higher Tmin relative to other regions for each season.

### 5.3 Trends in cloud fraction.

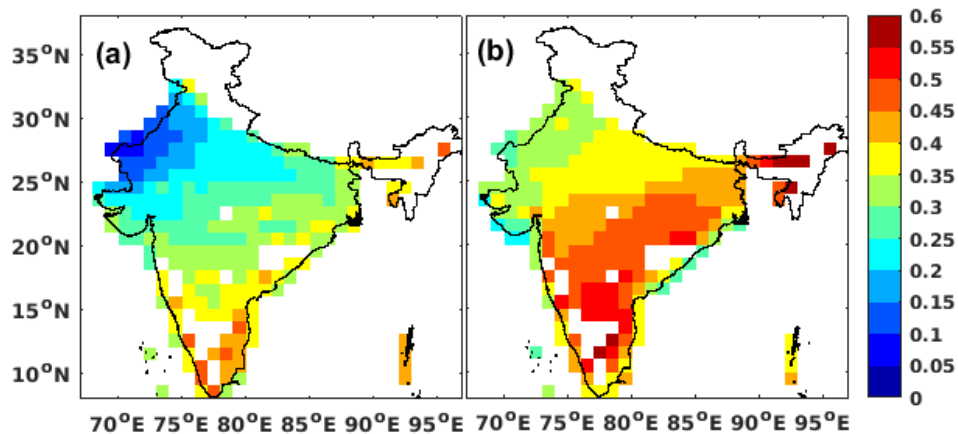


Fig 5.7: Spatial distribution of cloud fraction (2002-19) during (a) daytime (b) nighttime

During daytime, the cloud fraction is found to be 10-20% lower than the cloud fraction during nighttime which could be due to the lower nighttime temperatures facilitating formation of more clouds. The spatial patterns associated with both cloud fractions are, however consistent as clouds over a region are mostly driven by seasonal circulation which remains approximately constant through night and day. We can see a band of high cloud fraction area extending from the south in the North-East direction. We can see similar bands of lower cloud fraction to the north west of the high cloud fraction band. Interior regions are generally seen to have lower values of cloud fraction compared to the coastal areas which may lead to the surface temperature to be higher than normal during day time and lower than normal during the night.

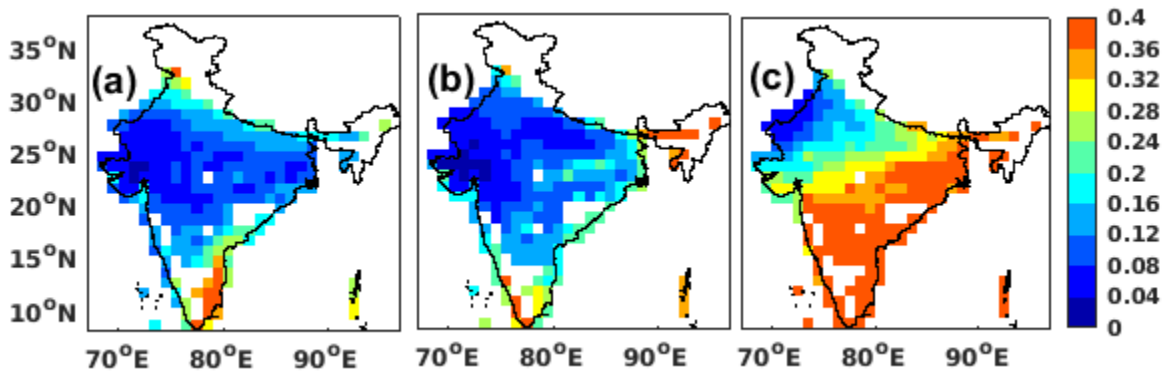


Fig 5.8: Spatial distribution of cloud fraction during daytime (a) DJF (b) MAM (c) SON.

The daytime cloud fraction during DJF is seen to be low (4-12%) over most of India, except for a small high cloud fraction region in southern India (which gets rain during the season from the retreating monsoon). The low cloud fraction could be due to the reduced energy reaching the surface during the season, inhibiting convection. We can see the cloud fraction increase during MAM due to the pre-monsoon convective activities, especially over the southern parts of India. We can see regions of high cloud fraction in the southwestern coast and northeastern India. The region of high cloud fraction increases further during SON to cover most of India (primarily a consequence of South-West monsoon and then retreating monsoon circulation). The cloud fraction is seen to be lowest over the northwest during the season.

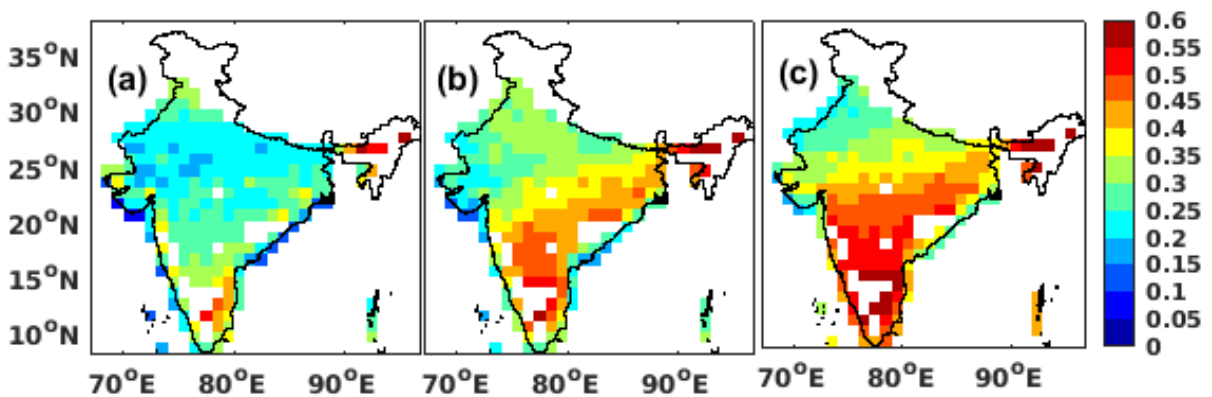


Fig 5.9: Spatial distribution of night time cloud fraction during (a) DJF (b) MAM (c) SON.



The spatial and temporal trends in the nighttime cloud fraction are consistent with the patterns seen in the daytime cloud fraction. However, the magnitude of cloud fraction varies and is seen to vary by as much as 10-20% over most of India which could be due to the prior discussed reasons.

#### 5.4 Trends in Total column water vapour.

The column water vapour is maximum over the coastal areas compared to the interior regions for daytime and nighttime. The spatial patterns of column water vapour are seen to be the same during both daytime and nighttime. However, the total column water vapour values are seen to be slightly higher during nighttime than daytime over the coasts.

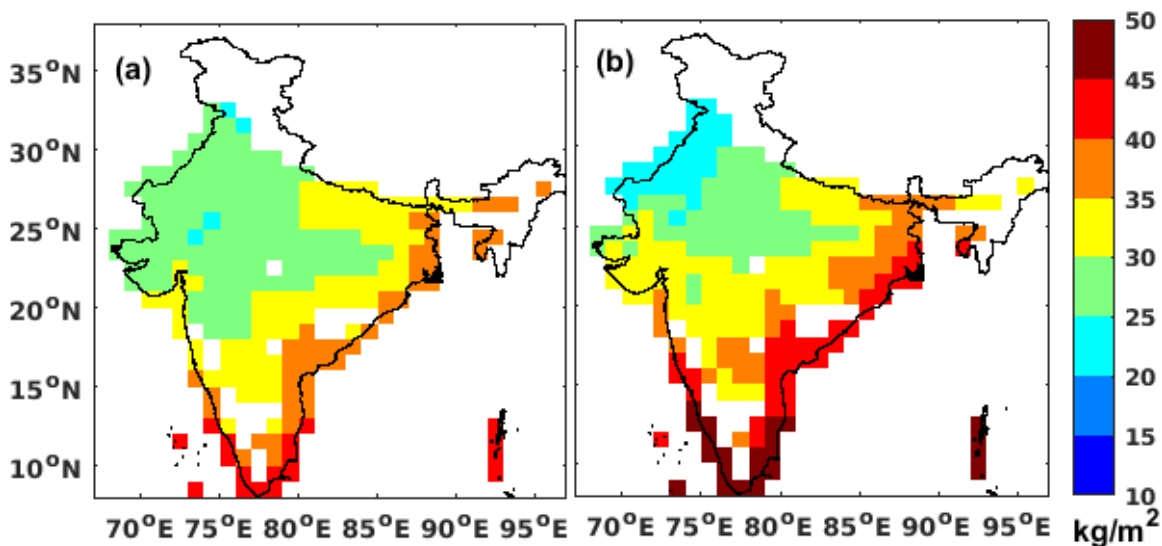


Fig 5.10: Spatial distribution of total column water vapour during (a) Daytime (b) Nighttime.

Total columnar water vapour content is minimum during the winter season, and becomes maximum during the pre-monsoon season. This is due to the higher air temperatures during the pre-monsoon season compared to the winter season. TWV starts decreasing shortly once the monsoon season is over, i.e. in the post-monsoon period.

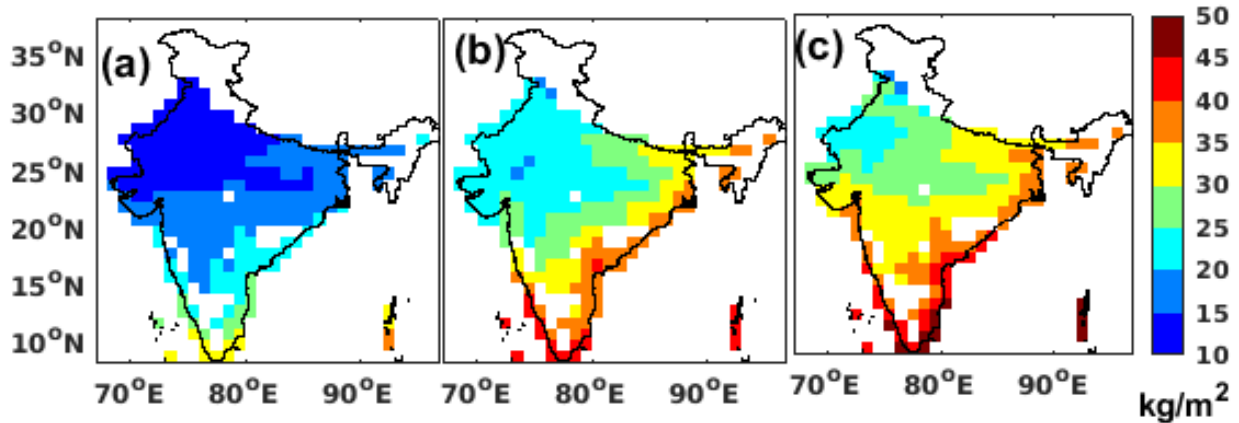


Fig 5.11: Spatial distribution of daytime total column water vapour during (a) DJF (b) MAM (c) SON.

The daytime and nighttime columnar water vapour are not seen to vary by much in spatial patterns as TWV is driven mostly by seasonal temperature variations. The nighttime columnar water vapour is observed to be slightly higher over certain regions due to the reduced air temperature during nighttime.

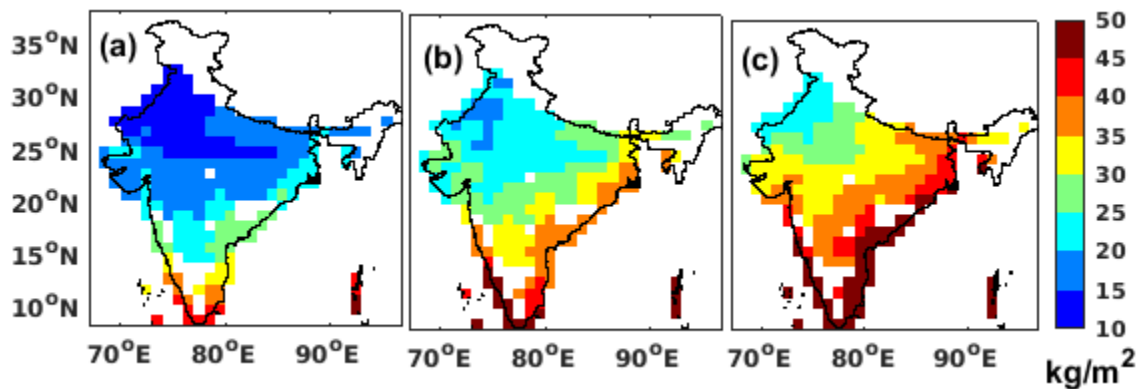


Fig 5.12: Spatial distribution of nighttime total column water vapour during (a) DJF (b) MAM (c) SON.

## 5.5 Trends in Angstrom Exponent (AE).

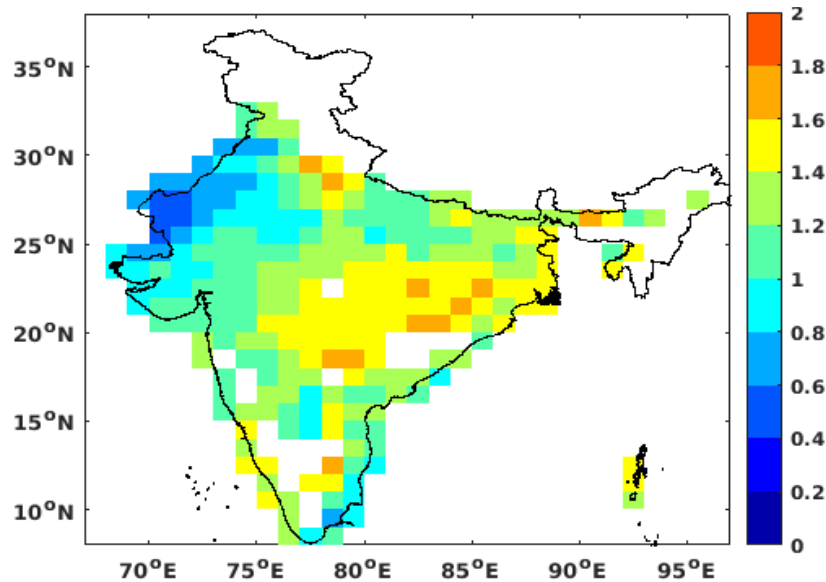


Fig 5.13: Spatial distribution of annual mean Angstrom Exponent

AE shows high values over central and eastern India. This is due to the presence of industries and a high population density which increases the fine mode anthropogenic aerosols over the region. The AE is lower over the coasts and over Northwest India, where coarse mode aerosols like sea salt and dust dominate. AE is moderate over the Indo-Gangetic plain owing to the region experiencing high loading of both anthropogenic (winter, post-monsoon) and natural dust (pre-monsoon).

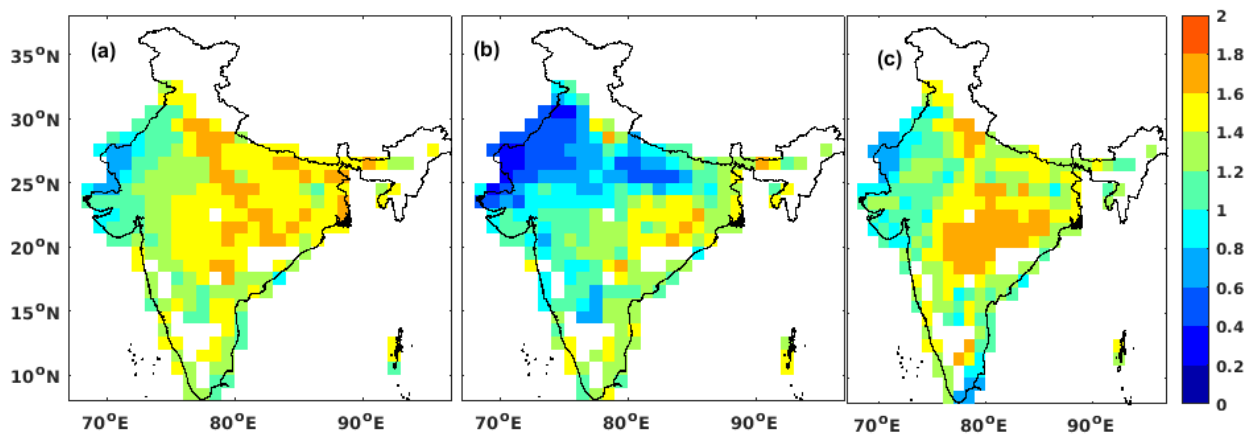


Fig 5.14: Spatial distribution of Angstrom Exponent during (a) DJF (b) MAM (c) SON.

The average AE is high during DJF, especially over the North Indian region. However, the AE drops over these regions due to the dust loading during MAM. Aerosols get washed out from the atmosphere during the monsoon, reducing the dust levels during the post-monsoon season. Thus we get the moderate AE during SON. It is to be noted that high AE exists over certain regions in central and eastern India during all seasons. These may also be related to the emissions from coal power plants over these regions and related mining activities.

## 5.6 Correlation analysis

### 5.6.1 Preliminary correlation analysis.

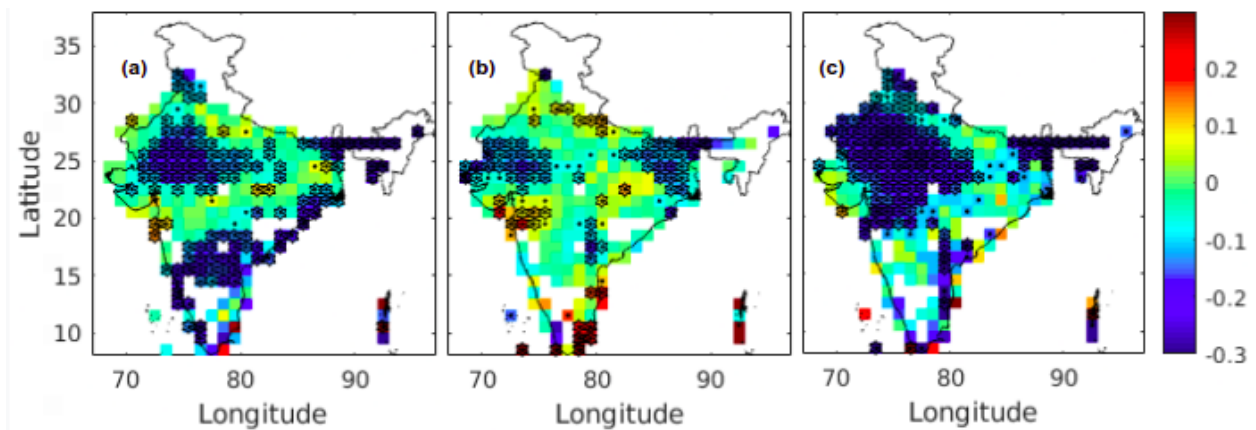


Fig 5.15: Correlation between aerosols and maximum surface air temperature (Tmax) (a) DJF (b) MAM (c) SON.

The correlation between aerosols and maximum surface air temperature during different seasons are surmised in Fig 5.15. We see an overall negative correlation between aerosols and surface air temperature over most of India during all seasons. However, it is to be noted that confounding variables like cloud fraction and total column water vapour might influence the relationship between aerosols

and surface air temperature. Therefore it is prudent to draw conclusions from the spatial plot of partial correlation between aerosols and surface air temperature while accounting for confounding variables like cloud fraction and column water vapour rather than the above figure.

### 5.6.2 AOD and Tmax correlation after accounting for CFR

Clouds can influence both shortwave and longwave radiation. During daytime, the clouds cool the surface by reflecting the shortwave radiation from the sun. From the partial correlation between AOD and Tmax, while accounting for CFR, we can see that the correlation between the variables is reduced in many regions. During DJF, in Fig 5.15.a we found a comparatively higher correlation than in Fig 5.16.a.

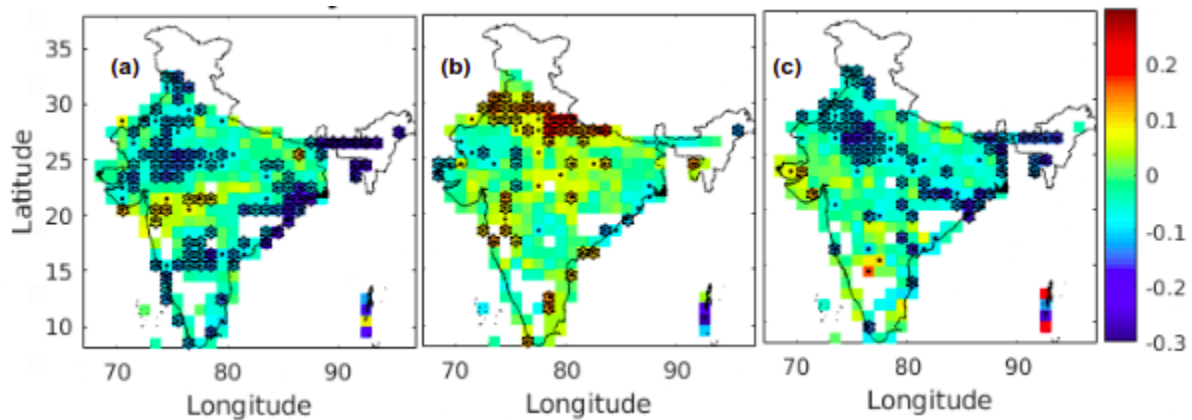


Fig 5.16: Correlation between aerosols and surface temperature when changes in cloud fraction are accounted for during (a) DJF (b) MAM and (c) SON.

Moreover, during MAM, we see slight negative to moderate positive correlation (Fig 5.16.b) compared to the negative correlation seen in Fig 5.15.b. It is seen that when we account for clouds, the correlation becomes positive in a lot of regions. We essentially see a large negative correlation region during SON showing lesser correlation when we account for cloud fraction. It is therefore assumed that the high correlation seen earlier could be due to the negative effect of clouds and gives us an indication that while studying aerosol effects on surface air temperature, it is imperative that we account for the effect of clouds.

### 5.6.3 AOD and Tmax correlation after accounting for CFR +TWV

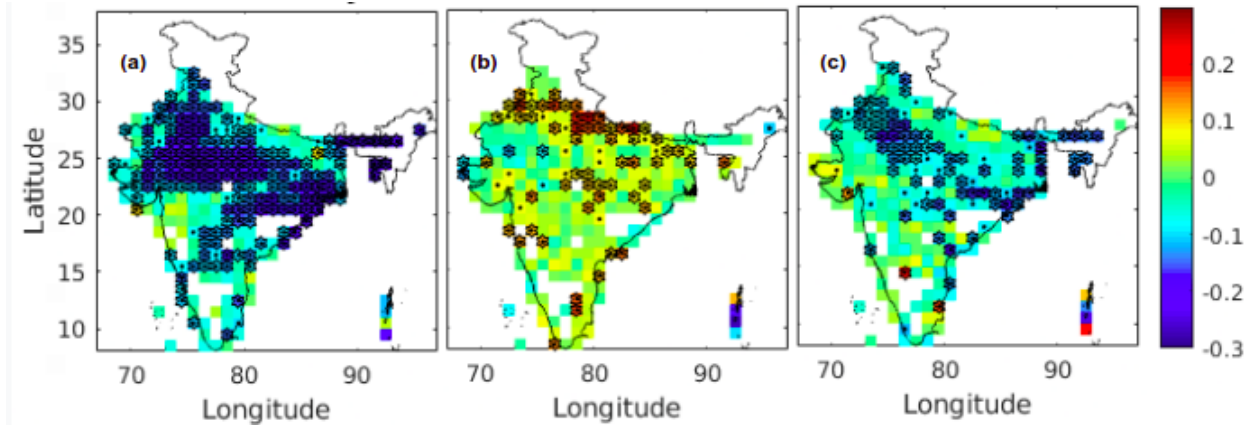


Fig 5.17: Correlation between aerosols and surface temperature when changes in cloud fraction and water vapour are accounted for during (a) DJF (b) MAM (c) SON.

The water vapour in the atmosphere can also interact with the radiation and influence the surface air temperature. A partial correlation between aerosols and surface air temperature while accounting for both cloud fraction and total water vapour in the atmosphere column reveals that many regions show a statistically significant relationship between the two study variables. During DJF, this effect is more pronounced as we can see that almost all of India has a statistically significant negative correlation between aerosols and surface air temperature. On the other hand, MAM shows a positive correlation throughout India (statistically significant in most of North India). At the same time, during SON, we can see a band over northern India with a statistically significant relationship between AOD and Tmax. The changes in TWV lead to changes in RH that changes particle size and thus AOD.

Thus, we can be positive that the water vapour and clouds need to be considered when studying the effects of aerosols on surface air temperature.

### 5.7 Regression analysis.

$\Delta AOD$  vs  $\Delta T_{max}$  in the preliminary region predicts a net cooling of  $-1.23$  °C/ unit AOD over the selected region. The average AOD over the region is  $0.44$ , implying a  $0.54$ °C cooling due to aerosols over the region during DJF. In a similar study done by Roy, 2008 the aerosols were seen to have standardised regression coefficients in the range of  $-0.6$  to  $-0.8$  over the region, which agrees closely with the values calculated in our study when our regression coefficients are standardised for the winter season, which in our case includes the month of December as well.

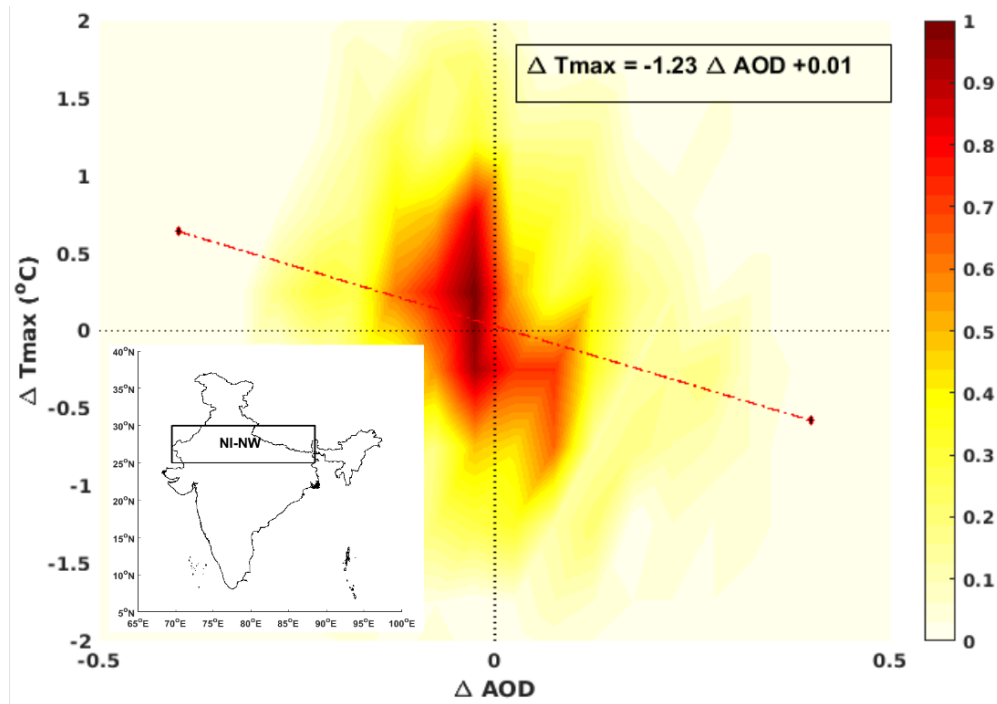


Fig 5.18:  $\Delta AOD$  vs  $\Delta T_{max}$ , over NI - NW.DJF, 2002-19. The figure is done for illustration purposes only. This can be done by restricting the data set to include points only when the changes in cloud fraction and column water vapour are minimal. This essentially lets us model it as a 1D problem. There is not much change in slope for this method and the multiple regression method, but this method leads to loss of data, making the prediction less robust.

### 5.7.1 Spatial patterns in aerosol effect for different seasons

The aerosol effect calculated at each grid point for each season lets us know if there is any seasonality or regional variations in the change in temperature due to aerosols.

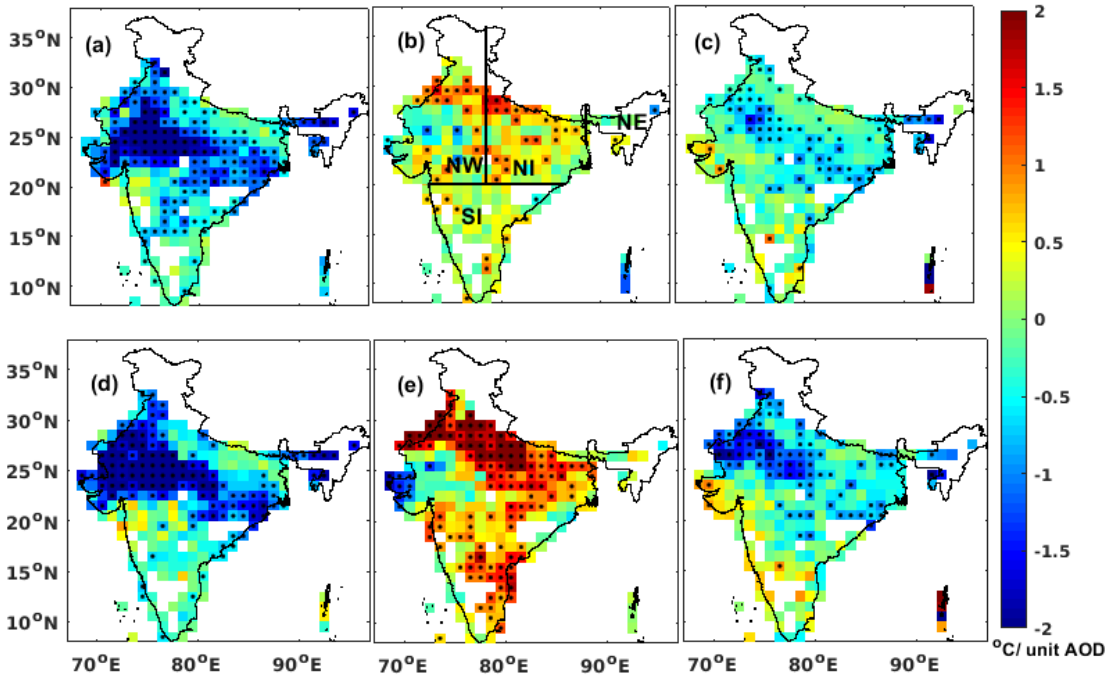


Fig 5.19: The spatial distribution of aerosol effect. The dots represent points which are statistically significant at 95%. (a) MODIS , DJF (b) MODIS, MAM. The markings show different regions took within India (c) MODIS SON (d) MERRA, DJF (e) MERRA, MAM (f) MERRA, SON

#### 5.7.1.1 DJF (Winter).

An explicit spatial and temporal nature to the effect of aerosols on surface temperature is observed. During DJF, the aerosols are seen to cool the surface to -1 to -1.5 ° C per unit AOD over most North India regions. A general nationwide cooling due to aerosols is observed during the season. One can see slight warming on the western coast around Mumbai, which could be due to the high amounts of anthropogenic aerosols such as black carbon prominent in the region (sometimes called the Bombay Plume). Black carbon can also increase the surface temperature through semi indirect effects by modulating the cloud processes (Koch and Delgenio, 2010). It is interesting to note that



the regions showing higher loading (IGP) show a lesser aerosol effect than other areas. This could potentially be due to the antagonistic effects of both absorbing (which includes black carbon) and scattering aerosols on surface temperature.

### 5.7.1.2 MAM (Pre-monsoon).

There is widespread warming due to aerosols during MAM over India. The effect is particularly prominent over N.I. ( $0.50\text{ }^{\circ}\text{C}$  / unit AOD). For unit AOD, the warming is in the range of  $0.03\text{ }^{\circ}\text{C}$  -  $0.97\text{ }^{\circ}\text{C}$  per unit AOD in N.I. and goes up to  $2\text{ }^{\circ}\text{C}$ /unit AOD over some regions in the N.W. However, we can also see isolated cooling over a significant portion of N.W.

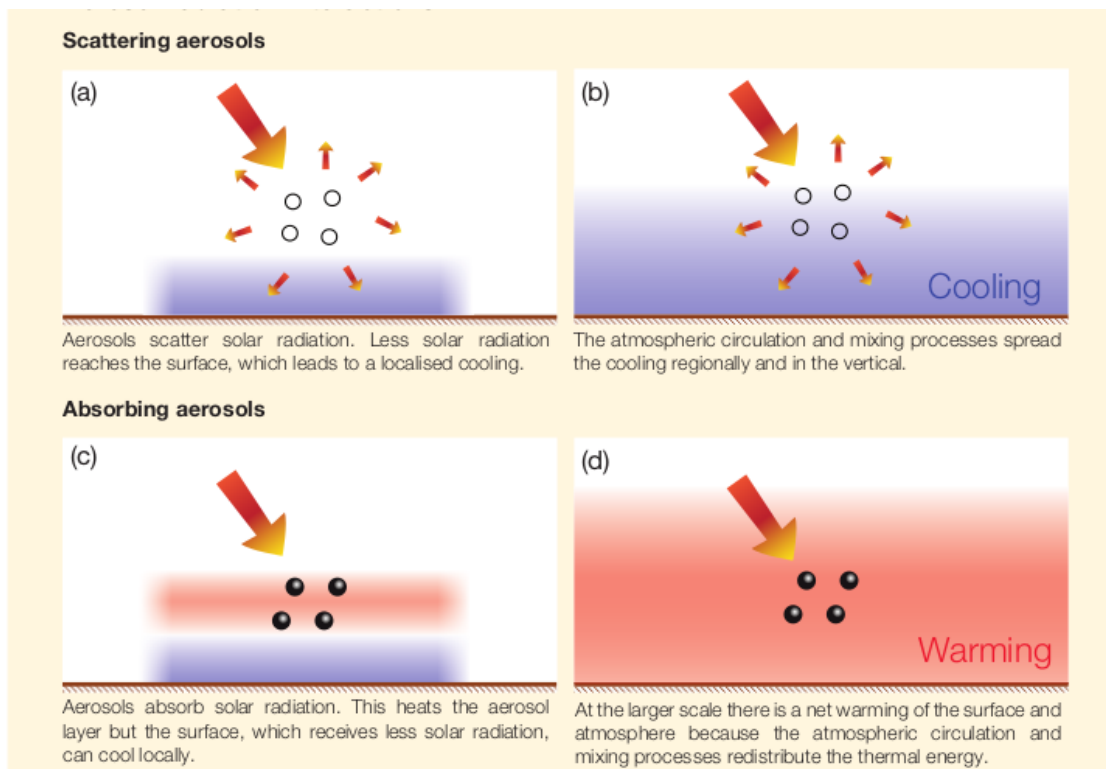


Fig 5.20: Potential mechanism as to how scattering aerosols cool the surface while absorbing aerosols warm the surface. Adapted from IPCC 2014 report

Contrary to popular belief, aerosols are found to warm up the surface more with more loading. This is hypothesised to be due to the large scale dust loading (which is an absorbing aerosol) over the region, as reported by Dave et al., 2020. The role of other

absorbing aerosols like black carbon (which are primarily anthropogenic) could also be significant, especially in the heavily populated IGP in warming the surface (Fig 5.20.c and Fig 5.20.d). Roy (2008) attributed the neutral to positive forcing seen in the pre-monsoon season to overcast skies trapping in longwave radiation. However, the warming signal persists even after including clouds in the regression leading us to believe that aerosols themselves have a warming effect as reported by Zhou and Savijarvi, 2014, Wang et al., 2017 and Garrett et al., 2002.

### **5.7.1.3 SON (Post monsoon).**

Aerosols are seen to cool the surface during the post-monsoon season. The AOD during the season is low compared to the pre-monsoon season due to the wet removal of aerosols during the monsoon season. Thus the aerosol effect is low compared to the winter season. The average cooling over most regions varies around  $-0.5$  °C/unit AOD, going as high as  $1$  °C/unit AOD over Northern India.

One can make out a band of statistically significant cooling starting to form extending from the Northwest to the eastern coast during SON. This band is seen to intensify during the winter season. The effect becomes positive during the pre-monsoon season, possibly due to increased dust loading amplified by high surface reflectance. Thus we can see clear seasonality in the observed aerosol effect.

### **5.7.2 Comparison between MERRA and MODIS results.**

The aerosol effect calculated using MERRA data shows the same general pattern as the ones calculated using MODIS data ie. aerosols cool the surface during DJF with maximum effect over NI and NW. The warming effect observed during MAM covers a broader region and is larger than the aerosol effect calculated using MODIS data. Aerosols cool the surface during SON in a similar pattern to the one computed using MODIS data.

It is to be noted that there is not much difference between the two during DJF and SON, but there is a considerable difference between the effects calculated in MAM. This could be due to MERRA amplifying the effects of absorbing aerosols which are present more during MAM. It is also to be noted that the regions where AE is high during DJF show comparatively lesser MERRA aerosol effect compared to the MODIS one.

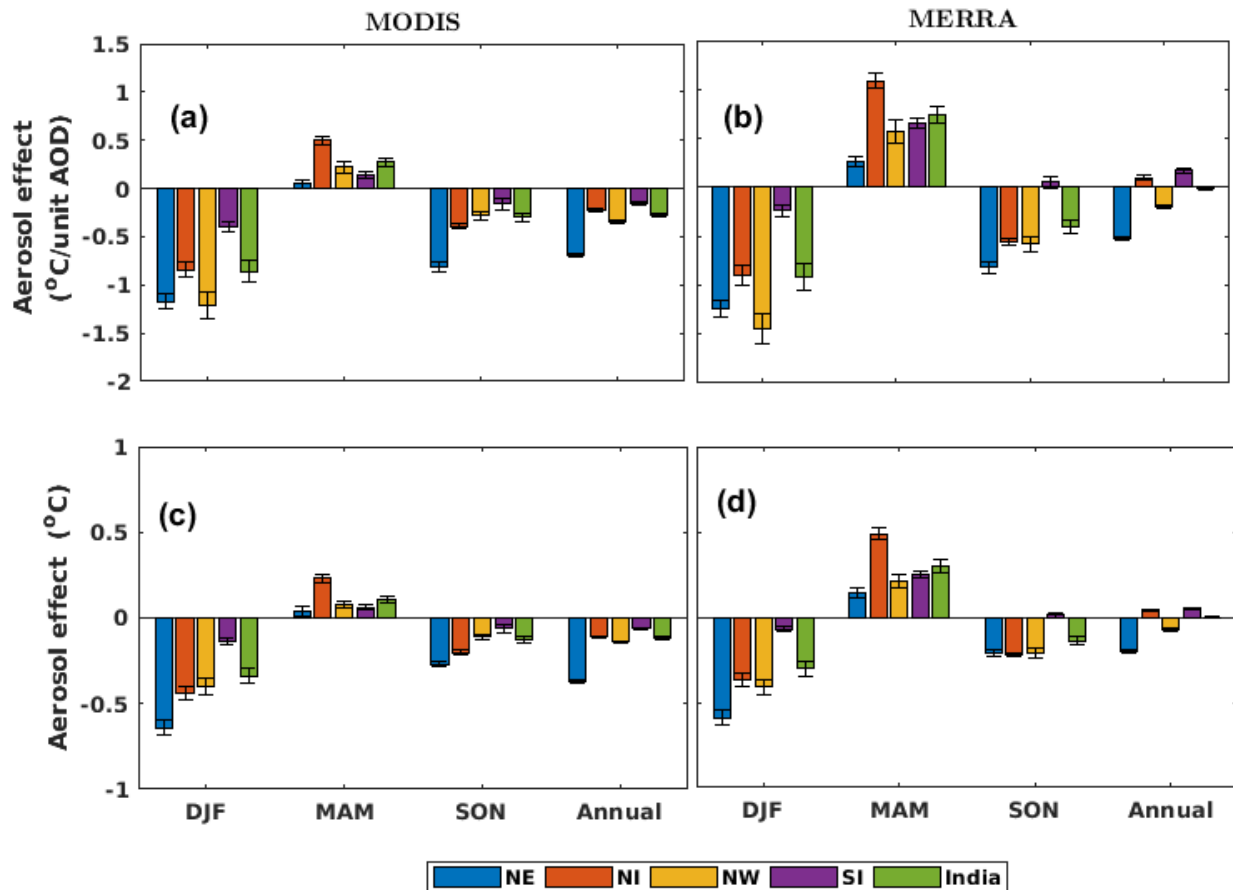


Fig 5.21: Region-wise aerosol effect (a) MODIS, slope (b) MERRA, slope (c) MODIS, actual temperature change (d) MERRA actual temperature change.

Most Northern India shows a statistically significant relationship between aerosol and surface air temperature compared to the south. This is consistent with the loading patterns where maximum loading is observed over northern India compared to the south. The MERRA aerosol effect generally tends to be slightly higher than the MODIS

one, but the seasonality described above holds for all regions. Aerosols are generally observed to cool the surface annually over all regions ( $-0.27^{\circ}\text{C}/\text{unit AOD}$ ). The efficacy of anthropogenic aerosols expected to be widespread during winter appears to be more in cooling the surface more per unit AOD than the natural dust aerosols that dominate during MAM and JJA. Therefore, additional effects may be compensating for the surface cooling when predominantly dust aerosol loading conditions prevail.

## 5.8 Sensitivity analysis.

### 5.8.1 Aerosol optical depth

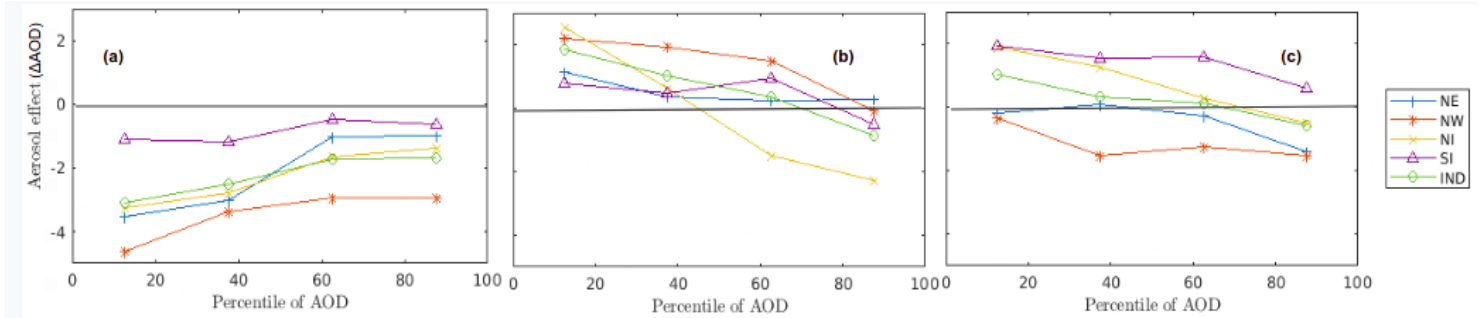


Fig 5.22: Sensitivity of aerosol effect ( $^{\circ}\text{C}/\text{unit AOD}$ ) to AOD (a) DJF (b) MAM (c) SON.

The aerosol effect seems to be becoming more negative as the aerosol loading increases except in DJF. During DJF, we see that the aerosol effect becomes more positive with increased loading. Absorbing aerosols like black carbon and organic carbon (mostly anthropogenic) could get trapped in the stable atmosphere and cause a rise in temperature with increased loading. This could also be why south India, with lesser population density and higher surface temperatures show a relatively lesser response to aerosol loading while the three regions to the north respond more to aerosol loading.

During MAM, we can see that the aerosol effect is positive at lower percentiles and becomes more and more negative at higher aerosol loading. The loading during this period is primarily due to dust. However, in contrast to the DJF season, the aerosol

effect becomes more and more negative with more loading. This shift is more apparent in NI and NW. This would suggest that dust, even though an absorbing aerosol, cools the surface at high loading conditions. The warming potential of anthropogenic BC and OC is seen to be more than that of dust.

The aerosol effect during SON becomes more negative with increased loading. Notably, regions like NI and SI have a positive aerosol effect at low loading even after the monsoons. However, the aerosol effect is negative for all regions at high loading.

Overall, more the aerosol loading, less the cooling or warming at the surface. The warming/cooling efficiency appears to be diminished relatively with increased aerosol loading conditions.

### 5.8.2 Angstrom Exponent

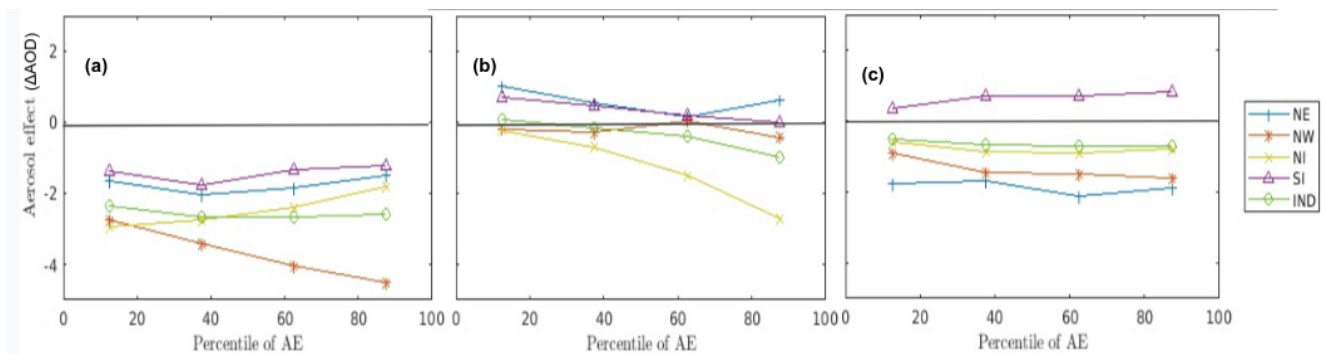


Fig 5.23: Sensitivity of aerosol effect ( $^{\circ}\text{C}/\text{unit AOD}$ ) to AE (a) DJF (b) MAM (c) SON.

Sensitivity studies to AE indicate that during DJF, the aerosol effect shows little response to changes in AE except in the northwest and north India. In the northwest we see the aerosol effect becoming more and more negative at higher AE percentiles, while we see the opposite in north India. This could be due to whether the anthropogenic aerosol is absorbing or scattering in nature. For example, absorbing anthropogenic aerosols might be causing the rise (more positive) in aerosol effect with increased AE in north India while scattering aerosols might be causing the aerosol effect to become more negative in the northwest.

During MAM, we see the aerosol effect being positive at smaller AE (potentially due to the coarser aerosols like dust being absorbing in nature) while becoming more and more negative at higher AE due to the finer anthropogenic aerosols cooling the surface. This is seen to be true over all regions.

The aerosol effect doesn't show much sensitivity to AE during SON. The AE during SON may have a smaller spread than the AE during other seasons due to the effect of the monsoon. This may make the aerosol effect more or less constant during this season as the values corresponding to the percentiles are closer to each other.

### 5.8.3 Maximum Temperature

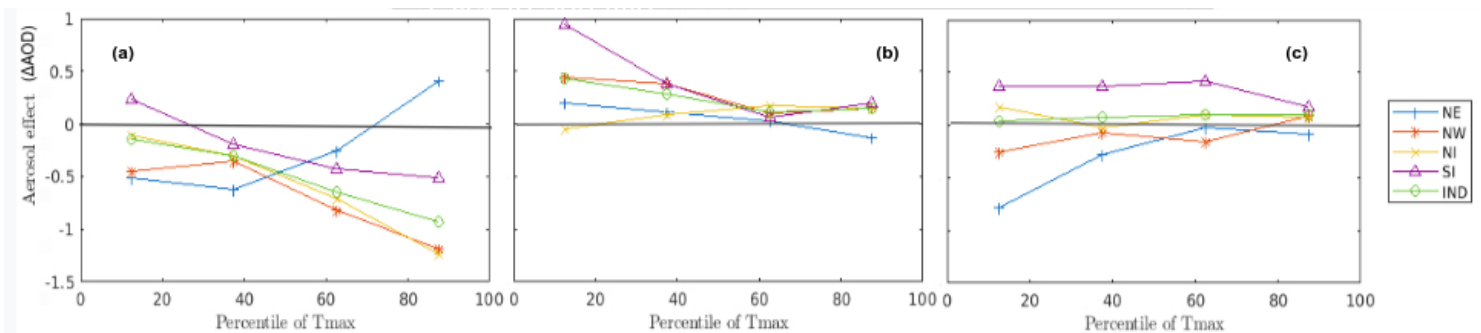


Fig 5.24: Sensitivity of aerosol effect ( $^{\circ}\text{C}/\text{unit AOD}$ ) to  $T_{\text{max}}$  (a) DJF (b) MAM (c) SON.

The aerosol effect is seen to have less sensitivity towards  $T_{\text{max}}$  changes than changes in AE and AOD. During the winter season, the aerosol effect seems to be becoming more and more negative with increasing temperature over all regions except the northeast. This could be due to the aerosols interacting with radiation more at higher temperatures, leading to more aerosol-induced cooling.

During MAM, the aerosol effect starts positive and gradually drops to zero.  $T_{\text{max}}$  has a negligible effect on the surface air temperature- aerosol relationship during SON and at higher temperatures, the relationship falls to zero. This leads us to believe that past a specific temperature, irrespective of the region, aerosols might have less effect on the surface air temperature.

The sensitivity of aerosol effect to Tmax reveals that lower maximum temperatures or cooler periods corresponds to warming effect due to aerosols, and warmer periods correspond to more cooling due to aerosols. This may indicate less convective or stagnant periods conducive to warming due to aerosols due to local high absorbing aerosols over highly polluted regions and vice versa.

### 5.9 Night time analysis.

During nighttime, we can see that the aerosols warm the surface in all seasons. The relationship is statistically significant over most of India during all seasons and covers almost all of India during MAM.

The warming during DJF is of the order of 1 - 2°C/unit AOD over a majority of the regions. Most of the warming pattern is concentrated in north, central India (mining and industrial regions of Bihar, Chattisgarh) and Gujarat. The MERRA observations show the same spatial pattern but indicate more substantial warming due to aerosols. The high intensity of warming around industrial areas suggests the increased influence of anthropogenic aerosols in driving the warming during the season.

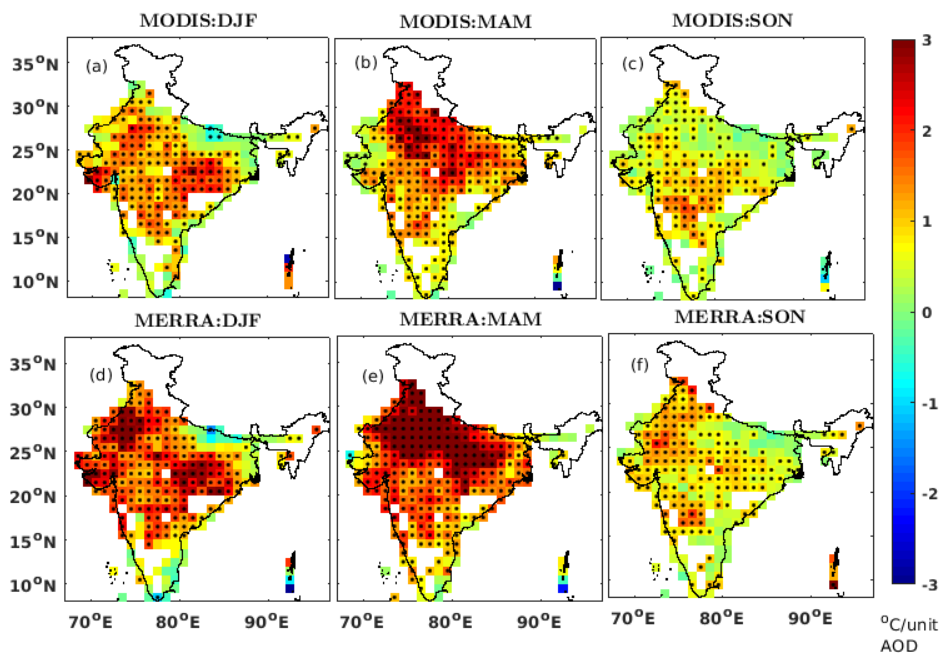


Fig 5.25: The spatial distribution of aerosol effect during night time. The dots represent points that are statistically significant at 95%. (a) MODIS, DJF (b) MODIS, MAM. The markings show different regions took within India (c) MODIS SON (d) MERRA, DJF (e) MERRA, MAM (f) MERRA, SON

The spatial extent of the warming increases both in scale and magnitude of warming during MAM. The regions close to the Thar desert and northern India show the maximum warming to the order of 2-3 °C/unit AOD. The enhanced warming during MAM could thus be due to the dust loading prevalent during the period. The warming extends all over India during MAM for the MERRA observations. The warming is generally greater than 3°C/unit AOD in most regions.

The warming subsides considerably during SON, possibly due to the lower aerosol concentration after washout during monsoon. The MERRA and MODIS results show considerable agreement in spatial extent and magnitude during this season. The results during night time also indicate that the reanalysis data can amplify the warming potential of absorbing aerosols.

#### **5.10 Daytime, nighttime & Net daily aerosol direct effect.**

The actual aerosol cooling/warming can be obtained by multiplying the average AOD of the season for a particular region. The MODIS and MERRA observations show that the aerosol effect during DJF over all regions during daytime is negative while it is positive during nighttime. This leads to the daytime and nighttime effects effectively cancelling each other. The net daily aerosol direct effect on surface air temperature ranges from -0.4 to 0.2 °C for MODIS and -0.3 to 0.3 °C for MERRA over most of India.

The aerosol effect during MAM for all regions is positive for daytime and nighttime. This leads to the overall effect being even more positive. The overall effect is in the order of 0.4 to 0.8 °C for MODIS, while it is in the range of 0.5 to 1.4°C for MERRA. Thus the



aerosols are expected to have a critical effect on the monsoon circulation over the region, which brings in rains critical for the country of almost 1.4 billion.

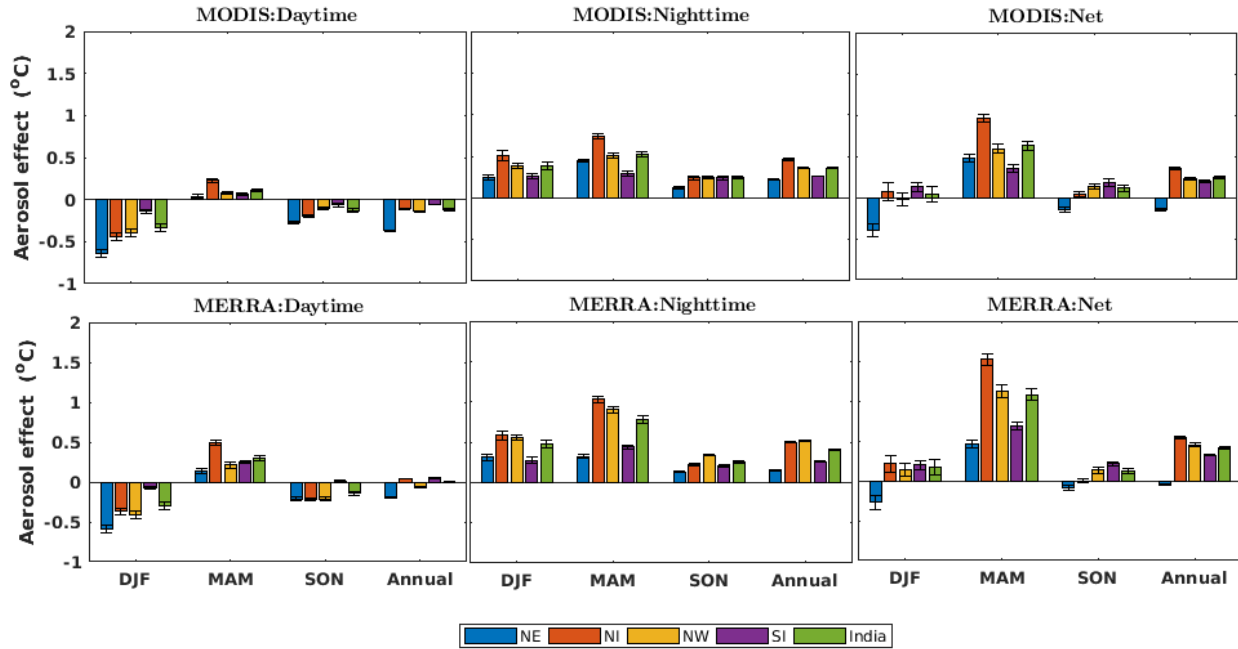


Fig 5.26: Region wise aerosol effect (a) MODIS, daytime (b) MODIS, nighttime (c) MODIS, net temperature change (d) MERRA, daytime (e) MERRA, nighttime (f) MERRA, net temperature change.

The aerosol effect for MODIS and MERRA during SON are closer in magnitude for both daytime and nighttime. The aerosol effect during night time is slightly more positive than the negative effect during daytime over all regions except NE. This leads to the net aerosol effect being in the range of -0.2-0.3 °C over most regions.

The annual net aerosol effect is seen to be modulated mainly by the aerosol effect during MAM and hence by the dust loading during the time. The annual aerosol effect during daytime is smaller compared to the aerosol effect during nighttime. This leads to the aerosol effect being positive over all regions except NE, where we see a slight negative effect. The aerosol effect is seen to vary between -0.2 - 0.4 °C over different regions for MODIS while being in the range -0.1 - 0.5 °C for MERRA annually over different regions.

## 5.11 Effects on the diurnal temperature range (DTR)

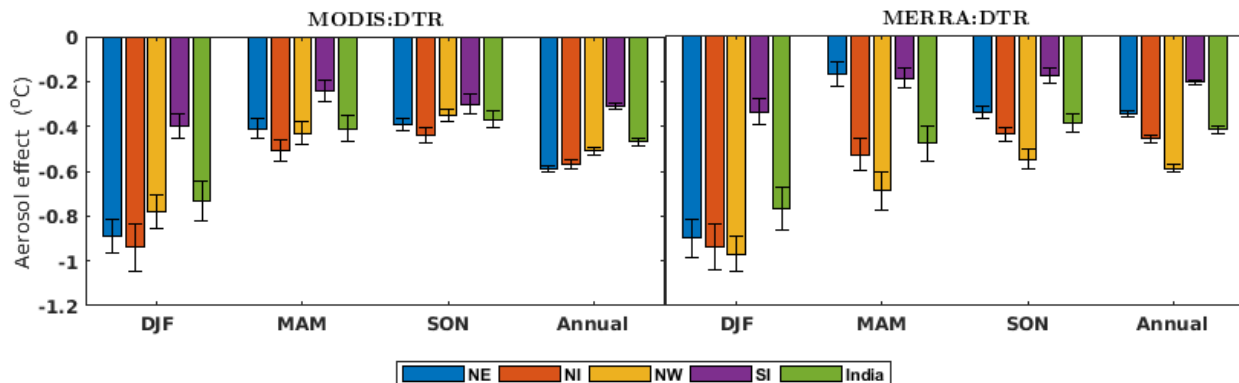


Fig 5.27: Region-wise aerosol associated DTR change (a) MODIS (b) MERRA

The DTR change is seen to be negative during all seasons, with maximum change during DJF as reported by Lal et al., 1996. The magnitude of DTR change is similar for both MODIS and MERRA during DJF. The results indicate that the DTR may be reduced by as much as 1°C over NI and NW and by at least 0.34 °C over SI.

The DTR change is lesser during MAM, with it varying between -0.55 - -0.2°C for MODIS and -0.2 - -0.7°C for MERRA. During SON, the aerosol effect on DTR is more or less close to each other for MODIS and generally varies around -0.4 °C for different regions. The DTR change calculated using MERRA shows a bit more variation, ranging between -0.2 - -0.6 °C.

NI and NW show the highest DTR change due to aerosols, while SI shows relatively lower aerosol associated DTR change. There is not much difference between annual DTR change due to aerosols calculated using MERRA and MODIS data. The annual DTR varies around -0.7 - -0.4 °C for MODIS and -0.7 - -0.3 °C for MERRA.

## 6 Summary and Conclusions.

Atmospheric aerosols are thus observed to have complex effects on surface air temperature based on the amount of loading, size, aerosol type (absorbing or scattering), etc. The most important results are summarised as follows.

1. Aerosols reduce the daytime surface temperature by as much as  $\sim -1.0$  to  $-1.5$   $^{\circ}\text{C}/\text{unit AOD}$  during winter and  $\sim -0.5$  to  $-1$   $^{\circ}\text{C}/\text{unit AOD}$  during the post-monsoon season over most of North India. Aerosols induce a warming of  $\sim 0.03^{\circ}\text{C}/\text{unit AOD}$  -  $0.97^{\circ}\text{C}/\text{unit AOD}$  over India's North-Western and northern parts. Absorption by predominantly dust aerosols and the highly reflective nature (surface albedo) of land surface during this period is speculated as possible causes. Aerosols cool the Indian region by  $-0.3^{\circ}\text{C}/\text{unit AOD}$  annually.
2. Nighttime analysis reveals an all seasons warming of  $\sim 1-2^{\circ}\text{C}/\text{unit AOD}$  during DJF and SON while being in the range of  $2-3^{\circ}\text{C}/\text{unit AOD}$  over most of India during MAM.
3. Analysis done using MERRA AOD data, a reanalysis dataset, was able to reproduce the spatial and temporal characteristics observed using MODIS data. In addition, sensitivity analysis reveals that the calculated aerosol modelled effect can change with aerosol loading and size.
4. Northern India shows a higher aerosol effect compared to southern India. This is consistent with the loading patterns where we see higher loading over the north Indian region.
5. The net daily aerosol effect is smaller during DJF ( $-0.4$  to  $0.2$   $^{\circ}\text{C}$  for MODIS ;  $-0.3$  to  $0.3$   $^{\circ}\text{C}$  for MERRA) and SON ( $-0.2-0.3$   $^{\circ}\text{C}$  for MODIS and MERRA) than MAM (large positive aerosol effect,  $0.4$  to  $0.8$   $^{\circ}\text{C}$  for MODIS;  $0.5$  to  $1.4^{\circ}\text{C}$  for MERRA) due to the similarity in signs of aerosol forcing during daytime and nighttime (overall addition). The aerosol effect is seen to vary between  $-0.2$  -  $0.4$   $^{\circ}\text{C}$  over different regions for MODIS while being in the range  $-0.1$  -  $0.5$   $^{\circ}\text{C}$  annually for MERRA over different regions.

6. Aerosols are also observed to reduce the diurnal temperature range (DTR) during all seasons. Annually, the DTR varies around -0.7 to -0.4 °C for MODIS. Similar results were obtained using the MERRA aerosol product.

## References.

D. Koch and A. D. Del Genio. Black carbon semi-direct effects on cloud cover: review and synthesis *Atmos. Chem. Phys.*, 10, 7685–7696, 2010. doi:10.5194/acp-10-7685-2010

Ramanathan, V., and Y. Feng, 2009: Air pollution, greenhouse gases and climate change: Global and regional perspectives. *Atmos. Environ.*, 43, 37–50.

Jones, A., Roberts, D. L., and Slingo, A.: A climate model study of indirect radiative forcing by anthropogenic sulphate aerosols, *Nature*, 370, 450–453, 1994.

Sen S. Roy (2008) Impact of aerosol optical depth on seasonal temperatures in India: a spatio-temporal analysis, *International Journal of Remote Sensing*, 29:3, 727-740, DOI: [10.1080/01431160701352121](https://doi.org/10.1080/01431160701352121)

Krishnan, R. & Ramanathan, V. Evidence of surface cooling from absorbing aerosols. *Geophys. Res. Lett.* 29, 54–56 (2002)

Albrecht, B., 1989: Aerosols, cloud microphysics and fractional cloudiness. *Science*, 245, 1227-1230.

A.K.Srivastava, M. Rajeevan, S. R. Kshirsagar(2009): : Development of High-Resolution Daily Gridded Temperature Data Set (1969-2005) for the Indian Region. *Atmos. Sci. Let.* (2009) DOI:10.1002/asl.232

Haywood J.M and Shine K.P. The effect of anthropogenic sulfate and soot aerosol on the clear-sky planetary radiation budget. *Geophysical Research Letters* 22,603-606(1995).

Deepshikha, S., Satheesh, S. K., and Srinivasan, J.: Dust aerosols over India and adjacent continents retrieved using METEOSAT infrared radiance Part I: sources and regional distribution, *Ann, Geophys.*, 24,37–61, <https://doi.org/10.5194/angeo-24-37-2006>, 2006.

Hsu, N.C., Jeong, M.J., Bettenhausen, C., Sayer, A.M., Hansell, R., Seftor, C.S., Huang, J., Tsay, S.C., 2013. Enhanced Deep Blue aerosol retrieval algorithm: The second generation. *J. Geophys. Res. Atmos.* 118, 9296–9315. <https://doi.org/10.1002/jgrd.50712>

Prasad, A.K.; Singh, R.P. Validation of MODIS Terra, AIRS, NCEP/DOE AMIP-II Reanalysis-2, and AERONET Sun photometer derived integrated precipitable water vapor using ground-based GPS receivers over India. *J. Geophys. Res. Atmos.* 2009, 114

Thomas S. Pagano, Moustafa T. Chahine, Hartmut H. Aumann, Baijun Tian, Sung-Yung Lee, Edward T. Olsen, Bjorn Lambrigtsen, Eric Fetzer, F. W. Irion, Xiuhua Fu, Wallace McMillan, Larrabee Strow, Chris Barnet, Mitch Goldberg, Joel Susskind, John Blaisdell, "Climate research with the atmospheric infrared sounder," *Proc. SPIE 6362, Remote Sensing of Clouds and the Atmosphere XI*, 63621K (12 October 2006); <https://doi.org/10.1117/12.689148>

Tian, B., E. Manning, J. Roman, H. Thrastarson, E. J. Fetzer, and R. Monarrez, 2020: AIRS Version 7 Level 3 Product User Guide. Available online at [NASA GES DISC AIRS Documentation Webpage](#).

Srivastava, A.K., Singh, S., Tiwari, S., Kanawade, V.P., Bisht, D.S., 2012. Variation between near-surface and columnar aerosol characteristics during winters and summers at a station in the Indo-Gangetic Basin. *J. Atmos. Solar-Terr. Phys.* 77, 57-66.

Twomey, S.A., 1974: Pollution and the planetary albedo. *Atmos. Env.*, 8, 1251-1256.

Twomey, S. A., 1977: The influence of pollution on the shortwave albedo of clouds. *J. Atmos. Sci.*, 34, 1149–1152.

Boucher, O., D. Randall, P. Artaxo, C. Bretherton, G. Feingold, P. Forster, V.-M. Kerminen, Y. Kondo, H. Liao, U. Lohmann, P. Rasch, S.K. Satheesh, S. Sherwood, B. Stevens and X.Y. Zhang, 2013: Clouds and Aerosols. In: *Climate Change 2013: The Physical Science Basis. Contribution of Working Group I to the Fifth Assessment Report of the Intergovernmental Panel on Climate Change* [Stocker, T.F., D. Qin, G.-K. Plattner,

M. Tignor, S.K. Allen, J. Boschung, A. Nauels, Y. Xia, V. Bex and P.M. Midgley (eds.)]. Cambridge University Press, Cambridge, United Kingdom and New York, NY, USA.

Christian A. Gueymard, Dazhi Yang, Worldwide validation of CAMS and MERRA-2 reanalysis aerosol optical depth products using 15 years of AERONET observations, *Atmospheric Environment*, Volume 225, 2020, 117216, ISSN 1352-2310, <https://doi.org/10.1016/j.atmosenv.2019.117216>.

Babu, S.S., Manoj, M.R., Moorthy, K.K., Gogoi, M.M., Nair, V.S., Kompalli, S.K., Satheesh, S.K., Niranjan, K., Ramagopal, K., Bhuyan, P.K., Singh, D., 2013. Trends in aerosol optical depth over Indian region: Potential causes and impact indicators. *J. Geophys. Res. Atmos.* 118, 11,794-11,806. <https://doi.org/10.1002/2013JD020507>

A. K. Srivastava, D. R. Kothawale, M. N. Rajeevan, Variability and Long-Term Changes in Surface Air Temperatures Over the Indian Subcontinent, *Observed Climate Variability and Change over the Indian Region*, 10.1007/978-981-10-2531-0\_2, (17-35), (2017).

P. Rohini, M. Rajeevan, A. K. Srivastava, On the Variability and Increasing Trends of Heat Waves over India, *Scientific Reports*, 10.1038/srep26153, 6, 1, (2016).

N. Naveena, G. Ch. Satyanarayana, A. Dharma Raju, K Sivasankara Rao, N. Umakanth, Spatial and statistical characteristics of heatwaves impacting India, *AIMS Environmental Science*, 10.3934/environsci.2021009, 8, 2, (117-134), (2021).

Rupakheti, D., Kang, S., Bilal, M., Gong, J., Xia, X., Cong, Z., 2019. Aerosol optical depth climatology over Central Asian countries based on Aqua-MODIS Collection 6.1 data: Aerosol variations and sources. *Atmos. Environ.* 207, 205–214. <https://doi.org/10.1016/j.atmosenv.2019.03.020>

M.T. Chahine, T.S. Pagano, H.H. Aumann, R. Atlas, C. Barnett, J. Blaisdell, L. Chen, M. Divakarla, E.J. Fetzer, M. Goldberg, C. Gautier, S. Granger, S. Hannon, F.W. Irion, R. Kakar, E. Kalnay, B.H. Lambrigtsen, S.-Y. Lee, J. Le Marshall, W.W. Mcmillan, L. Mcmillin, E.T. Olsen, H. Revercomb, P. Rosenkranz, W.L. Smith, D. Staelin, L.L. Strow, J. Susskind, D. Tobin, W. Wolf, L. Zhou AIRS: Improving weather forecasting and

providing new data on greenhouse gases Bull. Am.Meteorol.Soc.,87(2006),pp.911-926,[10.1175/BAMS-87-7-911](https://doi.org/10.1175/BAMS-87-7-911)

Jones, A., D.L. Roberts, and A. Slingo, 1994b: A climate model study of indirect radiative forcing by anthropogenic aerosols. *Nature*, 370,450–453.

J.T Kiehl and B.Briegleb (1993): The relative roles of sulphate aerosols and greenhouse gases in climate forcing, *Science*,260,311-314,1993

Kahn, B. H., Chahine, M. T., Stephens, G. L., Mace, G. G., Marchand, R. T., Wang, Z., Barnet, C. D., Eldering, A., Holz, R. E., Kuehn, R. E., and Vane, D. G.: Cloud type comparisons of AIRS, CloudSat, and CALIPSO cloud height and amount, *Atmos. Chem. Phys.*, 8, 1231–1248, <https://doi.org/10.5194/acp-8-1231-2008>, 2008.

Kaufman, Y.J., Tanré, D., 1998. Algorithm for remote sensing of tropospheric aerosol from MODIS. *NASA MODIS Algorithm Theory*. ... 85

Myhre, G. Consistency between satellite-derived and modeled estimates of the direct aerosol effect. *Science* **325**, 187-190 (2009).

Levy, R.C., Mattoo, S., Munchak, L.A., Remer, L.A., Sayer, A.M., Patadia, F., Hsu, N.C.,2013. The Collection 6 MODIS aerosol products over land and ocean. *Atmos. Meas.Tech.* 6, 2989–3034. <https://doi.org/10.5194/amt-6-2989-2013>

Milstein, A.B.; Blackwell, W.J. Neural network temperature and moisture retrieval algorithm validation forAIRS/AMSU and CrIS/ATMS.*J. Geophys. Res. Atmos.*2016,121, 1414–1430

Pandey, S.K., Vinoj, V., Landu, K., Babu, S.S., 2017. Declining pre-monsoon dust loading over South Asia: Signature of a changing regional climate. *Sci. Rep.* 7, 16062. <https://doi.org/10.1038/s41598-017-16338-w>

Gupta, P., Christopher, S.A., Wang, J., Gehrig, R., Lee, Y., Kumar, N., 2006. Satellite remote sensing of particulate matter and air quality assessment over global cities. *Atmos. Environ.* 40, 5880–5892. <https://doi.org/10.1016/j.atmosenv.2006.03.016>



Lal, M., et al. "Implications of Increasing Greenhouse Gases and Aerosols on the Diurnal Temperature Cycle of the Indian Subcontinent." *Current Science*, vol. 71, no. 10, 1996, pp. 746–752. JSTOR, [www.jstor.org/stable/24098730](http://www.jstor.org/stable/24098730).

Gupta, P., Khan, M.N., Silva, A., Patadia, F., 2013. MODIS aerosol optical depth observations over urban areas in Pakistan: quantity and quality of the data for air quality monitoring. *Atmos. Pollut. Res.* 4, 43–52. <https://doi.org/10.5094/APR.2013.005>

Platnick, S., Meyer, K. G., King, M. D., Wind, G., Amarasinghe, N., Marchant, B., et al. (2017). The MODIS cloud optical and microphysical products: Collection 6 updates and examples from Terra and Aqua. *IEEE Transactions on Geoscience and Remote Sensing*, 55(1), 502–525. <https://doi.org/10.1109/TGRS.2016.2610522>

Chunlei Wang, Bo-Hui Tang, Hua Wu, Ronglin Tang, Zhao-Liang Li. Estimation of Downwelling Surface Longwave Radiation under Heavy Dust Aerosol Sky. *Remote Sens.* 2017, 9, 207; doi:10.3390/rs9030207

Y. Zhou, H. Savijärvi. The effect of aerosols on longwave radiation and global warming. *Atmospheric Research* 135–136 (2014) 102–111

Kannemadugu Hareef Baba Shaeb. Aerosol Studies over Central India DOI: <http://dx.doi.org/10.5772/intechopen.85001>

Myhre, G., Myhre, C. E.L., Samset, B. H. & Storelvmo, T. (2013) Aerosols and their Relation to Global Climate and Climate Sensitivity. *Nature Education Knowledge* 4(5):7

Vinoj, V., S. S. Babu, S. K. Satheesh, K. K. Moorthy, and Y. J. Kaufman(2004), Radiative forcing by aerosols over the Bay of Bengal region derived from shipborne, island-based, and satellite (Moderate-Resolution Imaging Spectroradiometer) observations, *J. Geophys. Res.*, 109, D05203, doi:10.1029/2003JD004329.

V. Vinoj, S.K. Satheesh, and K. Krishna Moorthy (2010), Optical, radiative and source characteristics of aerosols at a remote island, Minicoy in the southern Arabian Sea, *Journal of Geophysical Research*, 115, D01201, doi:10.1029/2009JD011810.

